

Polyelectrolytes. Physicochemical Aspects and Biological Significance

MAGNUS ULLNER

1.1 INTRODUCTION

The basic facts about DNA are widely known and often repeated in general texts, for example, that its fundamental role is to store the blueprint for proteins, the machinery of life. The purpose of the Human Genome Project some years back was to read this information. Many people are also able to pick out the double helical DNA from molecular mugshots and explain that a key feature of the double helix is that it contains its own carbon copy, or rather a matrix of renewal by which the protein recipes are multiplied and handed down through the generations.

However, the situation is less clear when it comes to precise knowledge of how DNA behaves and interacts on the molecular level, for example, how DNA is neatly tucked away in the cell nucleus, or reversely how relevant genetic information is unraveled and presented to the translational machinery. A deeper understanding can be approached from two sides: from the specific chemical nature that makes DNA truly unique or from the generic properties of a larger group of molecules of which DNA is a member. This chapter is an introduction to the latter approach, focusing on the fact that DNA is a polyelectrolyte, as are many other biomolecules. Thus the purpose of this chapter is to discuss basic features of polyelectrolytes and to illustrate how they can be useful in a biological context in general, and not only where DNA is involved.

1.2 POLYELECTROLYTES AND BIOLOGICAL FUNCTION

A simple electrolyte or salt, such as NaCl, consists of positive and negative charges that can be separated when dissolved in water. The same is true for a polyelectrolyte, but the difference is that either the positive or the negative charges are joined together to form

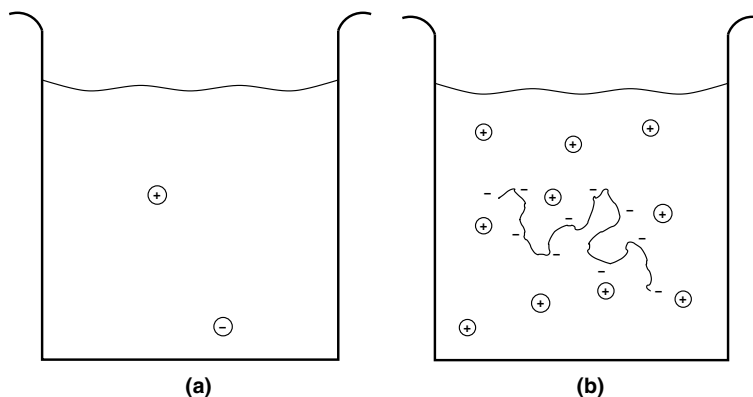


Figure 1.1 Dissociation of (a) a simple electrolyte and (b) a polyelectrolyte in an aqueous solution.

a highly charged molecule. This is illustrated schematically in Figure 1.1. Polyampholytes are also large charged molecules, but they contain both kinds of charges and can be net electroneutral. Polyelectrolytes and polyampholytes can be characterized as either strong (quenched), having a fixed charge distribution determined only by the chemical sequence, or weak (annealed), having charges that can move within the molecule and respond to the surrounding conditions, such as the pH of the solution. This is similar to characterizing an acid or a base as strong or weak. In other words, weak polyelectrolytes are weak polyacids or polybases and synthetic examples are poly(acrylic acid) and poly(vinylamine).

Many biomolecules are polyelectrolytes, and this is no coincidence because life on a molecular level is an aqueous solution of many components that need to be water soluble and interact in a controllable fashion. For example, proteins are usually polyampholytes with both acidic and basic groups, while DNA and RNA are strong polyelectrolytes.

Some of the naturally occurring polysaccharides are also polyelectrolytes, for example, alginates, hyaluronan, and pectin. There are also polyelectrolytes obtained by modification of natural polysaccharides, such as carrageenans and carboxymethylcellulose. Many polysaccharides (both charged and non-ionic) are used technically as thickeners, gelling agents, and emulsion stabilizers. In a biological context, they can serve similar functions, namely to generate structural viscoelastic elements. For example, hyaluronan is a major component in the vitreous body of the human eye, in synovial joint fluid, and in the comb of a rooster. The polysaccharides are too large to escape their compartment, and when they are charged, the counterions will be retained to maintain electroneutrality. For entropic reasons, water wants to enter the compartment to dilute its contents and the counterions boost the osmotic effect. The superabsorbents in diapers are polyelectrolyte gels, and they work in the same way. The high water content in the polysaccharide-rich parts of the body creates a gelatinous consistency, which may act as a shock-absorbing and lubricating material in the joints. “Viscoelastic water” is also a good way to fill a volume, especially if it needs to be clear as in the eye.

However, higher biological functions require a bit more than a modification of solution properties. To gain a more specific structure and functionality, hydrophobic groups are often needed, which can make it difficult to maintain the water solubility of the molecule and prevent aggregation, especially since the more advanced molecules need to be big. The solution to dissolution is to give these macromolecules a big dose of charge. This helps solubility not so much because each charge makes a molecule more hydrophilic but because it contributes a counterion that can explore the solution on its own and give the dissolved polyelectrolyte lots of entropy. More counterions means more entropy. Furthermore, charging the molecule can prevent aggregation by electrostatic repulsion, but it can also have the opposite effect when desired, by forming complexes with oppositely charged molecules. This can be large aggregates, such as DNA wrapping around histone complexes to form nucleosomes in chromatin, or small aggregates, such as ions binding to specific sites in proteins.

The electrostatic interactions are long ranged, as opposed to hydrophobic interactions, and they can be moderated. Weakly acidic or basic groups can have their charges turned on and off by shifts in the pH, and an increase in the ionic strength reduces the range of the electrostatic interaction, repulsive as well as attractive. The latter is the main salt effect if the ions that contribute to the ionic strength are monovalent. If there are multivalent counterions, correlations give rise to an attractive interaction between similarly charged objects or parts of the same molecule [1–10]. For example, DNA can be compacted with the so-called polyamines spermidine and spermine, which carry charges of +3 and +4, respectively [11–24]. Note that, in the context of polyelectrolytes, a better name for these polyamines would be oligoamines because they are rather small compared to the other molecules that we give the attribute “poly” to indicate that they are composed of many monomeric units. The polyamines are ubiquitous in prokaryotic and eukaryotic cells. They interact, for example, with DNA and RNA and have an essential role in cell growth and cell death, but much of their function on a molecular level remains unclear [25,26]. However, for the compaction of DNA the main effect is ion correlations, since other multivalent ions, such as $\text{Co}(\text{NH}_3)_6^{3+}$ [15,18,19,27–31], $\text{Cr}(2, 2' \text{ bipy})_3^{3+}$ [19], and Fe^{3+} [32], can also act as condensing agents and an excess of monovalent salt can decompact the molecules [9,13,15].

In short, by adding charge to molecules, nature gains an enormous amount of possibilities and life as we know it would be impossible without polyelectrolytes.

1.3 ELECTROSTATIC INTERACTIONS

1.3.1 Ion Distributions and the Poisson–Boltzmann Equation

For a highly charged polyelectrolyte at a finite concentration, it is not entirely true that the counterions wander off on their own; in fact the opposite charge still holds a mutual attraction that creates an ion atmosphere around the polyion. This is known as an electrical double layer and a common way to calculate the ion distribution is to use the

Poisson–Boltzmann (PB) equation,

$$\nabla^2\psi(\mathbf{r}) = -\frac{e}{\epsilon_r\epsilon_0} \sum_i z_i n_{i,0} e^{-\beta z_i e\psi(\mathbf{r})}, \quad (1.1)$$

where $\nabla^2 = \partial^2/\partial x^2 + \partial^2/\partial y^2 + \partial^2/\partial z^2$ is the Laplace operator, \mathbf{r} is the coordinate of a point in the solution, e is the elementary charge, ϵ_r is the dielectric constant of the solution, and ϵ_0 is the permittivity of vacuum. $\beta \equiv 1/k_B T$, with k_B being Boltzmann's constant and T the absolute temperature. $k_B T$ is a measure of the available thermal energy. The PB equation is obtained by relating the charge density $\rho_c(\mathbf{r})$ in the diffuse part of the double layer to the electrostatic potential $\psi(\mathbf{r})$ through Poisson's equation,

$$\nabla^2\psi(\mathbf{r}) = -\frac{\rho_c(\mathbf{r})}{\epsilon_r\epsilon_0}, \quad (1.2)$$

and making the approximation that the ion species i with valencies z_i are Boltzmann distributed with respect to the electrostatic potential without considering ion–ion correlations. This means that the local number density of ion i is

$$n_i(\mathbf{r}) = n_{i,0} e^{-\beta z_i e\psi(\mathbf{r})}, \quad (1.3)$$

where $n_{i,0}$ is the number density at a point where $\psi(\mathbf{r}) = 0$. Adding up $z_i n_i(\mathbf{r})$ for all ion species gives the distribution of net charge, $\rho_c(\mathbf{r})$, and transforms (1.2) into (1.1). The Poisson–Boltzmann equation represents a mean-field theory, since the ions in the diffuse part of the double layer only affect each other through their average contributions to the mean-field potential. Despite the simplifying neglect of ion–ion correlations, the PB equation is generally cumbersome to solve and even simple geometries require numerical solutions, except in special cases.

The equation itself is general. In order to solve it, a model with boundary conditions has to be defined. Since polyelectrolytes are somewhat extended and stiffened by the internal electrostatic repulsion, the usual choice of model is a charged cylinder. A straight cylinder might be a crude representation of thin, flexible polyelectrolytes, but it seems like a natural choice for DNA, which is stiff over contour lengths on the order of 500 Å and more or less has a cylindrical cross section with a radius of about 10 Å. Note, however, that very long DNA would qualify as thin and flexible.

With the Laplace operator written in cylindrical coordinates, the PB equation becomes

$$\frac{1}{r} \frac{d}{dr} \left(\frac{d\psi(r)}{dr} \right) = -\frac{e}{\epsilon_r\epsilon_0} \sum_i z_i n_{i,0} e^{-\beta z_i e\psi(r)}. \quad (1.4)$$

If the charge is smeared on the surface of the cylinder, the boundary condition for the potential at the surface, at $r = a$, is given by Gauss's law

$$\left. \frac{d\psi(r)}{dr} \right|_{r=a} = -\frac{\sigma}{\epsilon_r\epsilon_0} = \frac{e}{2\pi\epsilon_r\epsilon_0 a b}, \quad (1.5)$$

where σ is the surface charge density. The second equality represents a negatively charged surface with $\sigma = -e/2\pi ab$, where e/b is the linear charge density (a unit charge distributed over a length b) along the cylinder.

To treat a finite polyelectrolyte concentration, a cell model is often used, where the charged cylinder and surrounding ions are enclosed in a larger cylinder with a radius R , centered on the polyelectrolyte axis. The fact that the system is electroneutral gives a second boundary condition

$$\left. \frac{d\psi(r)}{dr} \right|_{r=R} = 0. \quad (1.6)$$

The electroneutrality also means that the net charge in the diffuse part of the double layer should have the same magnitude as the polyelectrolyte charge and the opposite sign,

$$2\pi \int_a^R \rho_c(r) r dr = -2\pi\sigma a = \frac{e}{b}, \quad (1.7)$$

which can be used as an alternative boundary condition. Once again the last equality is for a negatively charged surface.

The salt-free case, which is when the cell only contains the counterions that neutralize the surface, can be solved analytically [33,34]. Another special case, the Gouy-Chapman case, is a charged surface in equilibrium with a bulk salt solution. In the cell model this corresponds to letting R go to infinity with $\lim_{R \rightarrow \infty} \psi(R) = 0$ and $n_{i,0}$ representing the concentration of the bulk salt. This has to be solved numerically for a cylinder. Figure 1.2 shows the magnitude of the electrostatic potential outside a charged cylindrical shell at two charge densities and two bulk concentrations of salt, as well as the corresponding charge distribution in the diffuse part of the double layer. The radius of the cylinder is set to 10 Å. With the higher linear charge density of one unit charge every 1.7 Å, this roughly corresponds to DNA (upper curve in each pair in the figure), which is highly charged. The lower charge density is one unit charge per Bjerrum length, which is also a relatively high linear charge density. The Bjerrum length,

$$l_B = \frac{e^2}{4\pi\epsilon_r\epsilon_0 k_B T}, \quad (1.8)$$

is a measure of the strength of electrostatic interactions, depending on the dielectric constant, ϵ_r , and the temperature, T . In water at room temperature $l_B \approx 7.15$ Å.

Lowering the charge density obviously lowers the magnitude of the potential, but increasing the salt concentration also reduces the potential outside the cylinder, as can be seen in Figure 1.2, which shows the results for 10 mM (solid lines) and 100 mM (dashed lines) 1 : 1 salt. The charge density in the diffuse part of the double layer is due to the redistribution of ions, as shown in Figure 1.3. Although the coions contribute to a net charge by being repelled, the main effect is an increase in the counterion concentration in the neighborhood of the cylinder. Note that the volume of a cylindrical shell at a distance r from the cylindrical surface increases as r increases (the volume increases as $(a+r)^2$, where a is the cylinder radius), which means that the *number* of ions corresponding to a certain concentration is not as high close to the surface as

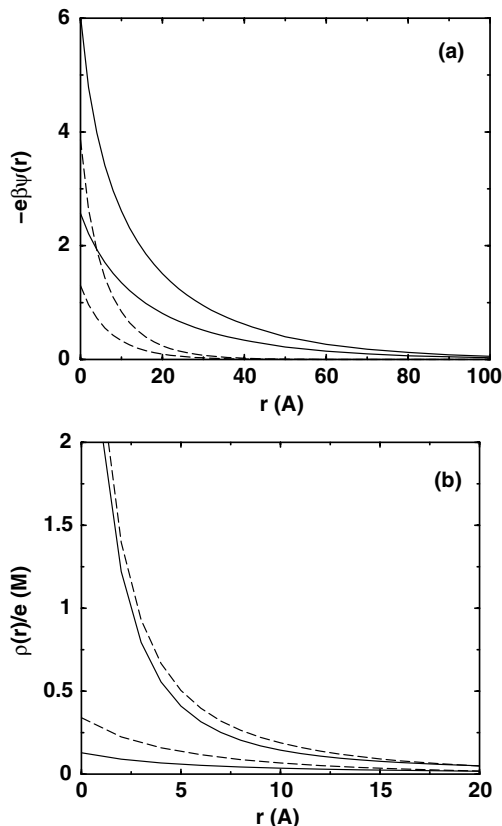


Figure 1.2 Poisson-Boltzmann results for the dimensionless electrostatic potential (a) and the neutralizing charge density (b) at a distance r from a negatively charged cylindrical surface with a 10 \AA radius in equilibrium with a bulk solution of a 1:1 salt. The salt concentrations are 10 mM (solid lines) and 100 mM (dashed lines). The upper curve in each pair corresponds to a linear charge density of one unit charge per 1.7 \AA , which corresponds to DNA, and the lower curve is for one charge per Bjerrum length (7.15 \AA).

further out. At higher salt concentrations there are more ions available, which makes the redistribution of ions to create a charge distribution less of a perturbation to the entropically preferred even ion distribution. The cylindrical charge can then be neutralized over a shorter distance and the double layer becomes thinner. The very existence of a double layer is an important characteristic of polyelectrolytes. For the cylinder it represents an effective radius, since the thickness of the double layer determines the range of the electrostatic interactions, and also because the ions in the diffuse part hinder the solvent when there is a flow. Both types of interactions affect the viscosity of the solution. We will return to this point later.

Yet another way to reduce the electrostatic potential is to increase the valency of the counterions, as illustrated by Figures 1.4a and 1.5a. These figures show comparisons between 1:1, 2:1, and 4:1 salts, where the bulk concentrations of

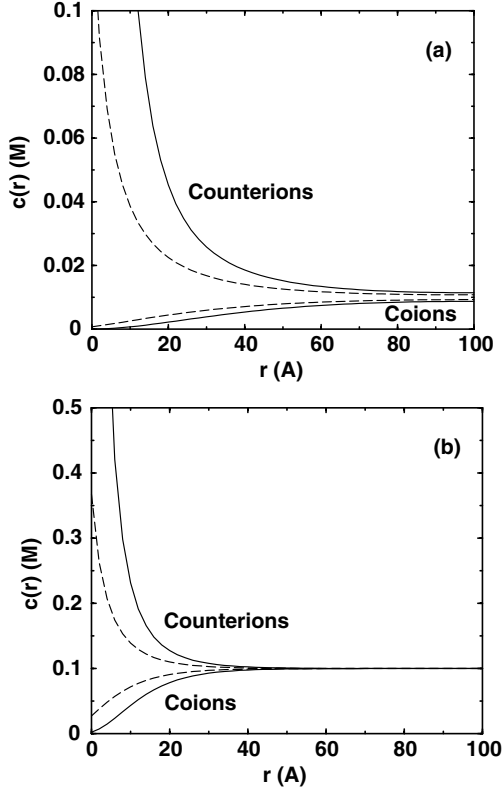


Figure 1.3 Poisson-Boltzmann results for the concentration of counterions (*upper curves*) and coions (*lower curves*) at a distance r from a charged cylinder with a 10 \AA radius in equilibrium with a 10 mM (a) and 100 mM (b) bulk solution of a 1 : 1 salt (Notice the difference in scale on the y-axes.) Solid lines correspond to a linear charge density of one unit charge per 1.7 \AA , which corresponds to DNA, and dashed lines one charge per Bjerrum length (7.15 \AA).

countercharges $|z_i|c_i$ are the same. The higher the valency, the larger is the amount of countercharge drawn close to the cylinder, and the neutralizing atmosphere becomes less extended, reducing the potential faster in terms of distance from the cylinder. It might be tempting to describe the effect as a result of increasing the ionic strength and put it on par with an increase in a 1 : 1 salt, since the ionic strength depends quadratically on ion valency,

$$I = \frac{1}{2} \sum_i z_i^2 c_i, \quad (1.9)$$

where c_i is the molar concentration of species i . However, the change in I would be the same if it were the coion valency that changed, but this has very little effect on the electrostatic potential and the charge distributions, as can be seen in Figures 1.4b and 1.5b. Another way to see the dominance of polyion-counterion interactions, as opposed to polyion-coion interactions, is by the fact that the counterion activity is

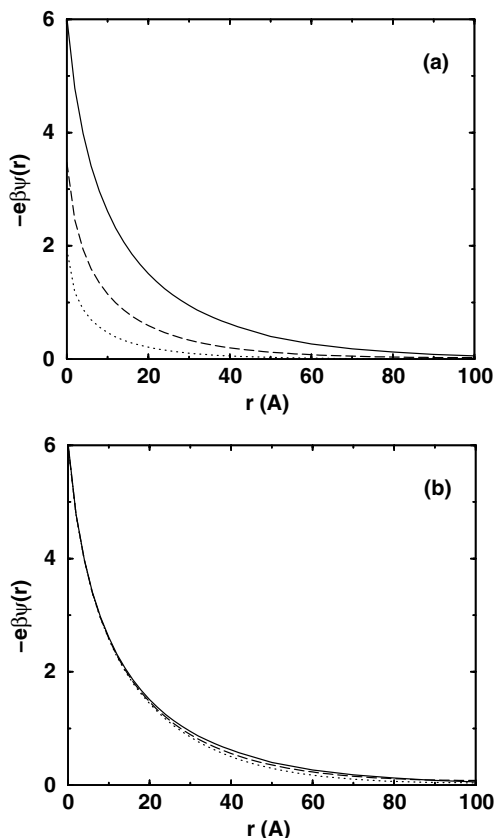


Figure 1.4 Poisson-Boltzmann results for the dimensionless electrostatic potential at a distance r from a negatively charged cylinder with a 10 \AA radius and a linear charge density of one unit charge per 1.7 \AA for (a) 1 : 1 (solid lines), 2 : 1 (dashed curves), and 4 : 1 (dotted lines) salts and (b) 1 : 1 (solid lines), 1 : 2 (dashed curves), and 1 : 4 (dotted lines) salts with bulk concentrations 10 mM, 5 mM, and 2.5 mM, respectively. In short, the valency of counterions (a) and coions (b) are varied, while the bulk concentrations of charges remain constant.

much more affected by the presence of the polyion than the coion activity. Simulations of polyelectrolytes with monovalent ions have shown that it is possible to define an effective ionic strength based on the counterion activity [35], as suggested experimentally by studies of polyelectrolyte viscosity using Manning theory to predict the proper ionic strength for the isoionic dilution method [36–39].

Although they serve to prove a point, the Poisson–Boltzmann results for multivalent ions should not be taken too literally. This is because the neglected ion–ion correlations become important for multivalent ions and higher concentrations. Modified Poisson–Boltzmann theory, which has also been applied to cylindrical geometry [40–42], strives to correct for the shortcomings of the original theory. Monte Carlo simulations have demonstrated that the modified theory is an improvement [43], but it comes at the cost of a more complicated set of equations.

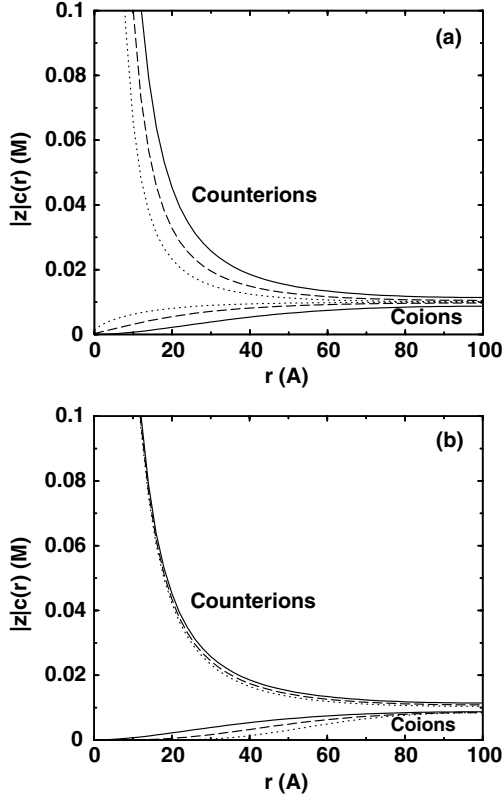


Figure 1.5 Poisson-Boltzmann results for the concentration of counterion charge (*upper curves*) and coion charge (*lower curves*) at a distance r from a charged cylinder with a 10 \AA radius and a linear charge density of one unit charge per 1.7 \AA for (a) 1 : 1 (*solid lines*), 2 : 1 (*dashed curves*), and 4 : 1 (*dotted lines*) salts and (b) 1 : 1 (*solid lines*), 1 : 2 (*dashed curves*), and 1 : 4 (*dotted lines*) salts with bulk concentrations 10 mM, 5 mM, and 2.5 mM, respectively. In short, the valency of counterions (a) and coions (b) are varied, while the bulk concentrations of charges remain constant.

1.3.2 Debye–Hückel Theory

If we dial back to monovalent ions and weak electrostatic potentials, the Poisson–Boltzmann equation may be linearized,

$$\nabla^2 \psi(\mathbf{r}) = \frac{e^2}{\epsilon_r \epsilon_0 k_B T} \sum_i z_i^2 n_{i,0} \psi(\mathbf{r}) = \kappa^2 \psi(\mathbf{r}). \quad (1.10)$$

This is the starting point for Debye–Hückel (DH) theory [44], and κ is known as the Debye screening parameter. In an excess of a 1 : 1 salt, which means that the concentration of the polyelectrolyte is so low that its own counterions can be ignored,

the Debye parameter can be expressed in terms of the salt concentration, c_s ,

$$\kappa^2 = \frac{e^2}{\epsilon_r \epsilon_0 k_B T} \sum_i z_i^2 n_{i,0} = 4\pi l_B \sum_i z_i^2 N_A c_i = 8\pi l_B N_A c_s, \quad (1.11)$$

where N_A is Avogadro's number. Note that κ^{-1} has the unit of length, and it is a measure of the range of the electrostatic interactions after the ion atmosphere has been taken into account. It is therefore often referred to as the screening length.

Within the Debye–Hückel approximation the cylindrical case can be solved analytically. The Debye–Hückel potential outside an infinitely long negatively charged cylinder of radius a is [45,46]

$$-e\beta\psi(r) = \frac{2l_B}{b} \frac{K_0(\kappa r)}{\kappa a K_1(\kappa a)}, \quad (1.12)$$

where b is the axial length per unit charge and $K_0(x)$ and $K_1(x)$ are modified Bessel functions of the second kind.

Figure 1.6 shows a comparison between the potentials obtained with the Poisson–Boltzmann equation and the Debye–Hückel approximation. For high charge densities and low salt concentrations, the latter performs poorly. This is because DH theory is a linear response theory, while the PB equation takes into account a nonlinear accumulation of counterions (see Figure 1.7), which reduces the electrostatic potential. For lower charge densities and higher salt concentrations, the nonlinear effects become less significant and the DH approximation becomes increasingly good. Expressed differently, lower charge densities and higher salt concentrations reduce the potential, which eventually makes the linearization of the PB equation a valid approximation.

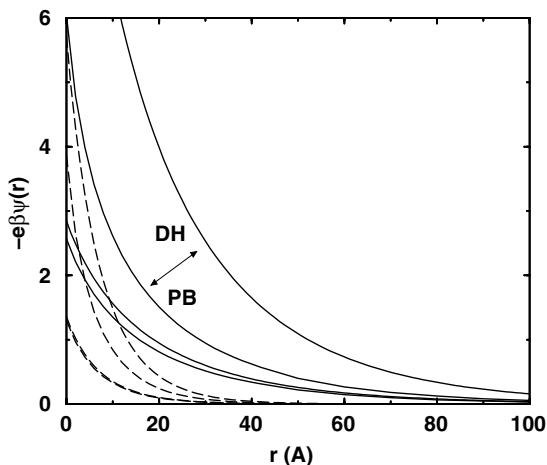


Figure 1.6 Same as Figure 1.2a, but with the Debye–Hückel results (*upper curve* in the related pairs) added for comparison.

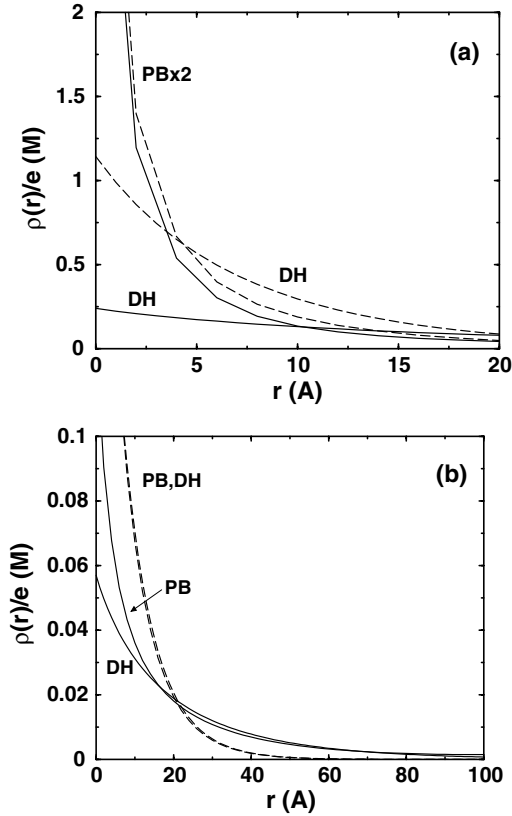


Figure 1.7 The Poisson–Boltzmann charge distributions from Figure 1.2*b* together with the corresponding Debye–Hückel results as marked. The linear charge densities are one unit charge per (a) 1.7 Å and (b) 7.15 Å.

Note, however, that higher salt concentrations also means more ion–ion correlations and when they are significant, the PB equation itself becomes questionable as an approximation.

With the computer power of today, it is not really a problem to calculate potentials and ion distributions around rigid geometries like a cylinder or even more detailed models of polyelectrolytes by solving equations numerically or by performing simulations. The great advantage of the DH approximation is instead in the study of flexible molecules.

The DH solution to the Gouy–Chapman case ($\lim_{R \rightarrow \infty} \psi(R) = 0$) for a sphere with radius a is

$$\psi(r) = \frac{ze e^{-\kappa(r-a)}}{4\pi\epsilon_r\epsilon_0 r(1+\kappa a)}, \quad (1.13)$$

where ze is the charge of the sphere. If we let $a \rightarrow 0$, we get the result for a point ion

$$\psi(r) = \frac{ze e^{-\kappa r}}{4\pi\epsilon_r\epsilon_0 r}, \quad (1.14)$$

which may be expressed as a pair potential for two point charges i and j ,

$$u_{ij}(r) = z_j e \psi_i(r) = \frac{z_i z_j e^2 e^{-\kappa r}}{4\pi\epsilon_r\epsilon_0 r} = k_B T z_i z_j \frac{l_B e^{-\kappa r}}{r}. \quad (1.15)$$

This is known as the screened Coulomb potential, and by comparison with the ordinary Coulomb potential,

$$u_{ij}(r) = k_B T z_i z_j \frac{l_B}{r}, \quad (1.16)$$

it is clear how κ , through the exponential factor, reduces the strength of the interaction and how κ^{-1} represents a length over which the (screened) electrostatic interactions remain significant. Furthermore, since (1.15) represents the interactions between two charges with their ion atmospheres taken into account and κ is a function of the salt concentration (see Eq. (1.11)), the screened Coulomb potential makes it possible to study salt effects without treating the free ions explicitly. For example, it is enough to express the conformational properties of a flexible polyion as functions of κ . This is why most theories for flexible polyelectrolytes use the Debye–Hückel approximation. It is also a great time-saver for simulations, since only the interactions between polyion charges have to be calculated to find the electrostatic energy when averaging over conformations.

However, as noted above, the Debye–Hückel approximation has its limitations. In particular, it cannot handle very large charge densities, which would produce a nonlinear accumulation of counterions. A common approach to deal with the nonlinearity, while retaining the simplicity of Debye–Hückel theory, is to apply Manning theory [47–50]. Conceptually it belongs to two-phase theories, where the polymer domain and the bulk solution are treated separately and ions may distribute themselves between the two “phases” [51–56]. There are two basic elements in Manning theory [57]. First, the linear charge density, expressed dimensionlessly as

$$\xi = \frac{l_B}{b}, \quad (1.17)$$

with b being the distance between unit charges, has a critical maximum value

$$\xi_{max} = \frac{1}{|z_1|}, \quad (1.18)$$

where z_1 is the valency of the counterions (assuming a single kind). Thus, for monovalent counterions, the maximum value is 1. If a polyion by itself has a higher charge density, a certain fraction of the counterions from the polyelectrolyte will be associated with the polyion, so that the combined charge density will be reduced to ξ_{max} . This is known as Manning condensation. Note that the “condensed” ions are not considered to be bound to sites on the polyion, only confined to a certain volume around it [48,49,50].

Second, the remaining counterions and other free ions from any added salt can be treated within the Debye–Hückel approximation given the effective charge of the polyion and its “condensed” counterions. For example, the interactions between charged sites on a highly charged polyion ($\xi > \xi_{max}$) are calculated with the screened Coulomb potential as if the polyion had a linear charge density of ξ_{max} and the concentrations of free ions that make up κ do not include the ions associated with the polyion. On the other hand, if the polyion is weakly charged ($\xi \leq \xi_{max}$), the Debye–Hückel approximation is used without modification.

From a theoretical point of view, the details of Manning theory, for example, the all-or-nothing association at a critical value of ξ , are open to debate [35,58–61] and Manning has responded to the criticism [50,57,62,63]. Regardless of the nature of its approximations, a theory can still be useful if it has the ability to predict experimental results. Manning has presented a number of experimental cases that show the critical behavior [62], and in comparison with experiments, the theory appears to be able to predict colligative properties, such as osmotic coefficients [47], but is much less successful in describing titration curves of polyelectrolytes [64,65], which involves intramolecular interactions. As was mentioned above, Manning theory has been able to produce counterion activities that successfully predict the proper ionic strength for the isoionic dilution method in studies of polyelectrolyte viscosity [36–39]. A problem is that a Debye–Hückel type of approach is not able to separate the activities of counterions and coions because the ions are lumped together in κ , and can at best give the mean activity coefficient. Simulations indicate that for certain concentrations and charge densities, the theory gives the correct value anyway, because of a cancellation of errors [35].

Applied to DNA condensation, Manning theory [66], or a modified version thereof [14], has been found consistent with experiment in that it gives a constant value of circa 90% for the degree of neutralization required to collapse DNA despite varying ionic conditions [14,15,17,18,27], although some variation in the theoretical neutralization as a function of ionic concentrations has also been observed [19]. Gel electrophoresis of DNA has also shown that the ratio of electrophoretic mobilities in the presence of multivalent counterions and monovalent, respectively, at the same ionic strength is in very good agreement with the ratio of the effective charge of DNA given by the theory [67]. It is sometimes mentioned that Manning theory, which only separates ions by valency, is not able to reproduce ion specific effects, such as the difference in efficiency between the trivalent polyamine spermidine and $\text{Co}(\text{NH}_3)_6^{3+}$ as condensing agents for DNA [15,18] (see Chapter 12 of this volume), but that would be to ask too much given the level of approximation.

To summarize, despite theoretical objections, Manning theory has proved useful as a simple way to calculate certain ionic effects, for example, colligative properties, at least in specific cases.

1.4 SOLUTION PROPERTIES

One of the main features of polymers in solution is that they have an effective size that is much larger than their mass would imply, compared to a compact sphere of a similar material. This is provided that they do not curl up to compact globules, of course, like

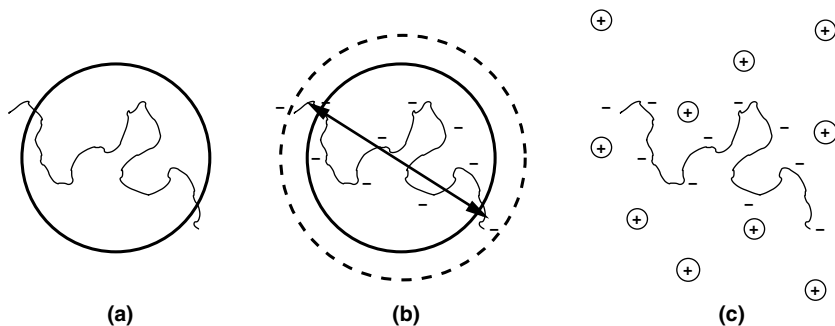


Figure 1.8 Schematic illustration of special features of charged polymers in solution: (a) Polymer, large effective size with low density; (b) electrostatic interactions extend the chain and increase the effective size with respect to other polyions; (c) counterions increase solubility and form the diffuse part of the electrical double layer (increase of effective dimensions with respect to the solvent).

most proteins do. A flexible chain whose segments are soluble explores different conformations, which means that it is on average rather spread out, and for polymer–polymer interactions and polymer–solvent interactions in a hydrodynamic context, it is the whole polymer domain that counts, as illustrated in Figure 1.8. Thus a small amount of material can increase the viscosity substantially. The effect is larger, the longer the polymer chain (i.e., the higher the degree of polymerization) because longer chains can explore larger volumes.

Another consequence is that polymer solutions have different concentration regimes, illustrated by Figure 1.9. In between the dilute and concentrated regimes, there is a special regime, known as the semidilute regime. The dilute and semidilute regimes are divided by the overlap concentration, defined as the point where the total concentration of the polymer solution is the same as in the polymer domain. The radius

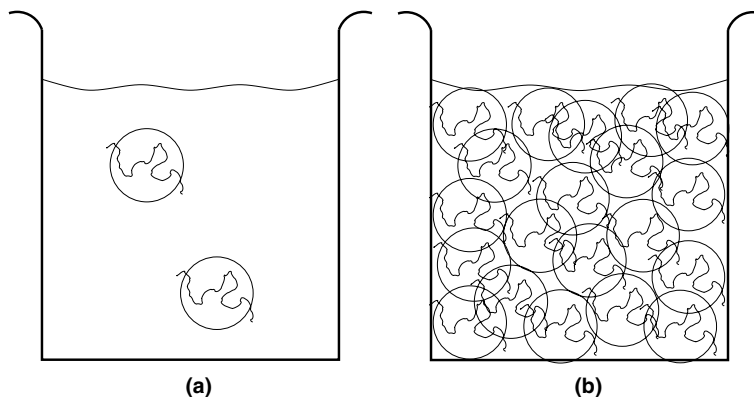


Figure 1.9 Schematic illustration of polymer solutions in (a) the dilute regime and (b) the semidilute regime close to the overlap concentration.

of gyration, R_G , is often used as a rough measure of the size of the polymer domain. An estimate of the overlap concentration, expressed as a monomer concentration, is then

$$c_p^* = \frac{3N}{4\pi R_G^3 N_A}, \quad (1.19)$$

where N is the number of monomers per chain or the degree of polymerization. Here it is assumed that N is known and c_p^* is expressed as a molar concentration, which is all right in theory and for the many biological molecules that are monodisperse. However, polymers in general are polydisperse, meaning they consist of a mixture of different chain lengths and then it is experimentally more convenient to replace N/N_A with an average molecular mass and express c_p^* as a mass concentration.

In the dilute regime the polymer domains are on average separated, and they interact as individual molecules. As the concentration is increased above the overlap concentration and the semidilute regime is entered, entanglements start to become significant while the characteristics of individual polymers, such as the degree of polymerization, start to become less important. An observable effect is that the viscosity increases faster as a function of concentration in the semidilute regime than in the dilute.

If charges are added, the internal repulsion will extend the chain and increase the polymer domain. At low ionic strength, when the screening length is on the order of the size of the polymer domain or larger, the electrostatic interactions will make the polymer–polymer interactions more long ranged, which can also be seen as an increase in the effective size. Both the increased size due to internal repulsion and the intermolecular interactions have been used to explain the polyelectrolyte effect observed in viscosity studies.

When neutral polymers are diluted, the reduced viscosity, η_r , decreases. It can, in general, be described by the linear Huggins equation [68],

$$\eta_r \equiv \frac{\eta - \eta_0}{\eta_0 c_p} = [\eta] + k_H [\eta]^2 c_p, \quad (1.20)$$

where η is the viscosity of the solution, η_0 that of the solvent, and c_p is the polymer concentration. The intrinsic viscosity, $[\eta]$, is by definition the reduced viscosity at infinite dilution ($c_p \rightarrow 0$) and is related to the size and shape of the molecule. For a sphere, the intrinsic viscosity is proportional to the radius, and in the nondraining case (when the molecule opposes a solvent flow as one big chunk and not as a collection of small, individually exposed units), a polymer may be treated as an effective sphere with $[\eta] \propto R_G^3$ [69,70]. The Huggins coefficient, k_H , was introduced as a fudge factor to allow for unknown intermolecular interactions characterizing the solute–solvent system [68], but for neutral polymers it is more or less a constant with a value in the range 0.3 to 1 [71].

On the other hand, when polyelectrolytes are diluted at low ionic strength, the reduced viscosity increases until a maximum is reached and then falls to $[\eta]$ at infinite dilution [72,73]. This is known as the polyelectrolyte effect. The increase in η_r at very

low ionic strength can be described using the empirical equation of Fuoss and Strauss [74,75],

$$\eta_r = \frac{A}{1+B\sqrt{c_p}}, \quad (1.21)$$

where A and B are fitting parameters. Although (1.21) gives a reasonable description of the increase in η_r on dilution, it obviously does not account for the existence of the maximum. As a consequence the intercept $1/A$ obtained by inverting the equation and plotting $1/\eta_r$ against $\sqrt{c_p}$, is not the intrinsic viscosity (η_r at infinite dilution) [76,77], which can be extrapolated from measurements at very low concentrations (after passing through the maximum) [78,79].

The classical explanation for the polyelectrolyte effect is that as the polyelectrolyte is diluted (and the counterions get more spread out), the electrostatic screening is reduced and the chain expands, obtaining an increasing effective size and thus a higher reduced viscosity [69,73]. The maximum occurs when the screening length goes far beyond the polymer domain and increasing it further does not have any effect on the intramolecular interactions. An alternative explanation is that it is the increasing intermolecular interactions that give rise to higher reduced viscosities [72,79–81]. This is favored by the fact that latices [82,83], telechelic ionomers with a charge at just one end [84], and spherical poly(styrenesulfonate) particles [85] all have a more or less fixed size but can still display a behavior similar to that of flexible polyelectrolytes. A pretty safe bet is that both types of interactions are important, with the intermolecular one dominating for short chains and intramolecular expansion increasing in significance as the degree of polymerization is increased [35].

By diluting the polyelectrolyte solution with a salt solution of a specific ionic strength, it is possible to get a linear decay of the reduced viscosity as described by the Huggins equation, but with a much larger value for the apparent Huggins coefficient ($k_H \gg 1$), as was first shown by Pals and Hermans [86,87]. This is called isoionic dilution. The rationale is that the specific salt concentration corresponds to an effective ionic strength, which is kept constant by the isoionic dilution. A constant ionic strength also means constant electrostatic interactions and therefore constant conditions for both the conformational interpretation of the polyelectrolyte effect and the intermolecular explanation, leading to a linear Huggins-type behavior. We have already mentioned the fact that the effective ionic strength is coupled to the counterion activity [35] and that Manning theory has been used successfully to predict the effective ionic strength for vinylic polyelectrolytes [36–39], although the application of the theory is not entirely correct from a strictly theoretical point of view (see above) [35].

The electrical double layer also influences viscosity because the shearing forces distort the ion atmosphere, giving rise to energy dissipation and an increased viscosity. This is known as the primary electroviscous effect, and it depends both on the ionic strength and the shear rate. The effect can be observed as a change in $[\eta]$ as a function of these factors. The intermolecular interactions between polyelectrolytes produce the secondary viscous effect, which can be observed as very large values of the Huggins coefficient.

1.5 FLEXIBILITY

The solution properties just described are affected by chain flexibility. They are to a certain extent even a direct consequence of this flexibility, even though the electroviscous effects, for example, can also be observed for polyelectrolytes with more or less fixed shape, such as spherical and rodlike polyelectrolytes.

A different aspect of flexibility is the ability of linear molecules to bend locally to interact with more globular ones. A very important biological example is the winding of DNA around histone complexes to form nucleosomes (discussed in detail in Chapters 6 and 7 of this volume). Another is the packing of DNA inside a viral capsid. If a molecule is treated as a uniform, flexible rod, the total elastic bending energy can be written as [88]

$$E_{\text{bend}} = \frac{k_B T l_{bc}}{2} \int_0^L \left(\frac{d\mathbf{u}(s)}{ds} \right)^2 ds = \frac{k_B T l_{bc}}{2} \int_0^L \bar{\rho}(s)^2 ds = \frac{k_B T l_{bc}}{2} \int_0^L \frac{1}{R(s)^2} ds, \quad (1.22)$$

where $\mathbf{u}(s)$ is a unit vector in the direction of the molecule at a point s along the line describing the molecular contour. The change in direction $d\mathbf{u}(s)/ds$, which describes the curvature, corresponds to a vector $\bar{\rho}(s)$ in the plane of bending and perpendicular to $\mathbf{u}(s)$, in other words, normal to the molecular line at s . The magnitude of $\bar{\rho}(s)$ is the inverse of the radius of curvature $R(s)$. For a uniformly bent rod, that is, when the radius of curvature is a constant $R(s) = R_0$, the integral is trivial, and the result is

$$E_{\text{bend}} = \frac{k_B T l_{bc} L}{2R_0^2}. \quad (1.23)$$

The bending coefficient l_{bc} represents the local mechanical properties of the molecule. Since it is a measure of stiffness and has the unit of length, it is also known as a persistence length.

1.5.1 The Concept of Persistence Length

The wormlike chain, introduced by Kratky and Porod [89], is a model that is able to describe a molecule with local stiffness that becomes increasingly flexible as the molecule is made longer. The model is characterized by an exponentially decaying orientational correlation function,

$$C(s) = e^{-s/l_{oc}}, \quad (1.24)$$

where l_{oc} is the characteristic length that describes the decay, namely the orientational correlation length, also known as persistence length. The latter term is more widespread, but it is also something of a Trojan horse, familiar on the outside but harboring

potential confusion within. The problem is that persistence length can be defined in no less than four different ways [90]. The definitions are all equivalent for a wormlike chain in three dimensions and have therefore been used interchangeably as explanations for what is meant by persistence length. However, as soon as we leave the confines of the one-parameter model, the separate definitions start to represent different properties and display diverging behavior. This is most notable for polyelectrolytes, which have long-range interactions, but it is enough with short-range interactions, as long as they can act through space and not just sequentially along the chain.

To understand the pitfalls of persistence length as a conformational measure, we start with the orientational correlation function, which is a measure of how much the direction of the chain changes over a certain distance along the contour. This is represented by the average projection of one bond on another as a function of the contour distance between them (the number of bonds times the bond length), as illustrated in Figure 1.10, where the direction of the first bond in (a section of) a chain is used as the reference direction. Furthermore the chain in the figure is composed of discrete bonds, while the wormlike chain is, in principle, a smooth continuous chain without kinks. In this case the bond vectors are unit vectors showing the direction of the tangent to every point along the chain (compare with the text following Eq. (1.22)). The parameter s in (1.24) represents the distance along the contour between such points. Thus, if we allow the chain to fluctuate and plot the average projection of the bond vectors on the reference bond as a function of contour separation, we get the orientational correlation function.

If the interactions that determine the change in direction of the chain are localized to short segments (i.e., there are no interactions between distant parts of the chain), it is easy to show that the orientational correlation function becomes exponential as in (1.24) [91]. This condition is fulfilled by the model represented by (1.22), which is a chain described as a bendable rod with a local bending energy inversely proportional to the square of the radius of curvature [88]. It can be shown that a chain with only this type of energy has an orientational correlation function like (1.24); that is, it is wormlike, with $l_{oc} = l_{bc}$ [88,92].

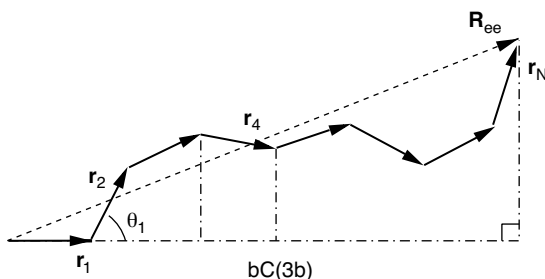


Figure 1.10 Chain represented as bond vectors, r_i , with a fixed length b . R_{ee} is the end-to-end vector. $bC(3b)$ is the average length of the projection of bond vector r_4 , with $C(3b)$ being the value of the (dimensionless) orientational correlation function for a separation of 3 bonds.

Note that the equality holds in three dimensions. For a chain bound to a surface, the relationship is $l_{oc} = 2l_{bc}$ [93–95]. The difference is in the energy–entropy balance that produces an average bond angle. In two dimensions, a bond vector like \mathbf{r}_2 in Figure 1.10 describes a circle when it explores all bond angles θ (θ_1 in the figure) and without an energetic bias, all angles have the same probability or weight in the average. In three dimensions, the bond maps out the surface of a sphere and the points on the surface have equal probability in the absence of energetic contributions. For a given angle θ the rotation around the axis of \mathbf{r}_1 draws a circle on the spherical surface, and this circle increases as θ increases from 0 to $\pi/2$ (0° to 90°) and decreases again between $\pi/2$ and π (90° and 180°). Thus, when there is an energetic penalty that wants to keep angles close to 0, the greater weight (proportional to the circumference of the circle of rotation) associated with angles in the direction of $\pi/2$ will increase the average bond angle compared to the two-dimensional case. The bond angle is connected to l_{oc} through

$$e^{-b/l_{oc}} = \langle \cos \theta \rangle, \quad (1.25)$$

where b is the bond length and $\langle \dots \rangle$ represents the averaging. For small angles and bond lengths

$$\frac{b}{l_{oc}} = \frac{\langle \theta \rangle^2}{2}, \quad (1.26)$$

since

$$e^{-x} = 1 - x + \dots \quad (1.27)$$

for $x \ll 1$ and

$$\cos \theta = 1 - \frac{\theta^2}{2} + \dots \quad (1.28)$$

for $\theta \ll 1$. The latter set of equations applies to the wormlike chain because it is a continuous chain. For a continuous chain it is possible to choose a contour length $s = b \rightarrow 0$, which also leads to $\theta \rightarrow 0$, where θ is the angle between tangent vectors \mathbf{u} at points a length s apart.

To calculate the average in (1.26), the energy as a function of θ is required. For a chain bending in one plane with a constant radius of curvature R , $\theta = s/R$, and the bending energy obtained from (1.22) for a contour length b is

$$E_{\text{bend}} = \frac{k_B T l_{bc}}{2b} \theta^2. \quad (1.29)$$

In the small angle limit this leads to

$$\langle \theta^2 \rangle = \frac{b}{l_{bc}} \quad (1.30)$$

in two dimensions [93–95], which with (1.26) gives $l_{oc} = 2l_{bc}$. In three dimensions the bending in different planes has to be considered, and the result is [88]

$$\langle \theta^2 \rangle = \frac{2b}{l_{bc}}, \quad (1.31)$$

producing $l_{oc} = l_{bc}$.

An important point is that the dimensionality difference is a result of the fluctuations in the bond angle under the influence of an energy that gives a nonzero $\langle \cos \theta \rangle$. If the bond angle is fixed, the dimensionality does not affect averages such as the root-mean-square radius of gyration, as long as there is free rotation around the bonds, because these rotations cancel out [91]. In other words, for a wormlike chain the expressions for conformational averages, for example, (1.33), are the same for a given l_{oc} regardless if the chain explores a three-dimensional or a two-dimensional space.

For real molecules that are free in solution, it is generally hard to probe the local details, which is necessary to determine the orientational correlation function or the local bending energy experimentally. However, electron microscopy and atomic force microscopy (AFM) can produce highly magnified images of molecules on two-dimensional substrates, more precisely on grids and surfaces, respectively. Usually the molecules are transferred from a solution to the grid/surface via an adsorption step. By tracing the contours, correlation functions can be measured and, for example, be compared to the wormlike-chain model to give a local persistence length. DNA fragments have been investigated this way with both electron microscopy [93,96–98] and AFM [94,95] as well as in thin liquid films using cryo-electron microscopy [99]. Electron microscopy has also been used to study polysaccharides [100]. Depending on whether the adsorbing conditions allow the molecules to equilibrate on the surface, the contours can be most consistent with the behavior of a chain in two dimensions or a projection of a three-dimensional chain [94]. The latter is an approximation, since a mathematical projection shortens the contour length, while the contour length is preserved for a real molecule.

Mechanical properties can be studied by applying a force to stretch the molecule and measure the extension, as has been done to DNA with the help of magnetic beads [101,102], flow [103], and laser tweezers [104–107]. Since the whole molecule is stretched, a model [101,102,104,108–112] is required to interpret the results in terms of local properties, such as l_{bc} and the stretch modulus. The latter measures the resistance to increasing the contour length and becomes important at large degrees of stretching [104–106]. Generally, the models are based on either a freely jointed chain

or a wormlike chain. For double-stranded DNA the wormlike chain gives the best agreement with the form of the force-extension curves [102,105,110,113]; for single-stranded DNA, an extensible freely jointed chain has proved adequate [104].

A more common experimental approach to study persistence length is to measure global properties related to molecular size, such as the radius of gyration or the intrinsic viscosity. Local parameters can theoretically be extracted from the global measurements by comparing the latter to model calculations. For example, the root-mean-square radius of gyration, R_G , can be obtained by integrating over the orientational correlation function

$$R_G^2 = \frac{2}{L^2} \int_0^L ds' (L-s') \int_0^{s'} ds (s'-s) C(s), \quad (1.32)$$

and by inserting (1.24), we get the result for a wormlike chain

$$R_G^2 = \frac{l_{oc}L}{3} - l_{oc}^2 + 2\frac{l_{oc}^3}{L} - 2\frac{l_{oc}^4}{L^2} (1 - e^{-L/l_{oc}}), \quad (1.33)$$

which for very long chains ($L \gg l_{oc}$) becomes

$$R_G^2 = \frac{l_{oc}L}{3}. \quad (1.34)$$

It is common practice in light scattering, for example, to use these equations to extract a persistence length from a measured radius of gyration. However, if the molecule is not a wormlike chain (and real molecules usually are not), the result will not be the orientational correlation length but something different (see the next section), a form of persistence length that we may call projection length, l_p [90]. The reason for the name is that the simplest integral over the orientational correlation function

$$l_p = \int_0^L C(s) ds \quad (1.35)$$

corresponds to the projection of the end-to-end vector on the direction of the first bond. This is also illustrated by Figure 1.10, since it is clear that summing the projections of the individual bonds gives the projection of the end-to-end vector. For an infinitely long wormlike chain we have

$$l_p = \int_0^\infty e^{-s/l_{oc}} ds = l_{oc}. \quad (1.36)$$

Projection length is actually a common name for a group of definitions, all of which involve integration over the orientational correlation function. Expressing projection length as the projection of the end-to-end vector on the direction of the first bond is the most direct definition of these.

Another common way to express persistence length is as “half the Kuhn length.” This is also a form of projection length because it is linked to another global quantity that can be obtained from the orientational correlation function by integration, the root-mean-square end-to-end distance, R_{ee} . For a freely jointed chain, which is simply a random walk, composed of N segments of length b , we have

$$R_{ee}^2 = Nb^2 = Lb, \quad (1.37)$$

where $L = Nb$ is the contour length. Since the freely jointed chain is a basic model for a polymeric molecule, the idea is that the real molecule can be represented by an effective freely jointed chain, such that

$$R_{ee}^2 = N_K l_K^2 = Ll_K, \quad (1.38)$$

where a second condition $L = N_K l_K$ has been used in the last equality. l_K is called the Kuhn length, and N_K is the number of Kuhn segments. To see the connection to persistence length, we need the end-to-end distance of a wormlike chain,

$$R_{ee}^2 = 2 \int_0^L (L-s)C(s) ds = 2 \int_0^L (L-s)e^{-s/l_{oc}} ds = 2l_{oc}[L - l_{oc}(1 - e^{-L/l_{oc}})]. \quad (1.39)$$

When $L \gg l_{oc}$ this becomes

$$R_{ee}^2 = 2Ll_{oc}, \quad (1.40)$$

and we immediately see the connection to (1.38) with $l_{oc} = l_K/2$. Since we have integrated over the correlation function again, the persistence length coupled to the end-to-end distance is better expressed as a projection length and we should write $l_p = l_K/2$.

In the other limit, $L \ll l_{oc}$, (1.39) becomes

$$R_{ee}^2 = L^2, \quad (1.41)$$

which is the expression for a straight rigid rod. The fourth definition of persistence length is the crossover distance, l_{cd} , which represents the contour length where the two types of limiting behavior meet, if they are extrapolated to intermediate chain lengths. Thus, if we set $L = l_{cd}$ and equate (1.40) and (1.41), we get

$$l_{cd} = 2l_{oc}. \quad (1.42)$$

There is a trivial factor of 2 separating the crossover distance from the persistence length of a wormlike chain. It could have been included in the definition to make all definitions truly equivalent for the basic model in three dimensions, but it makes no difference for a qualitative discussion.

At the same time as they introduced the wormlike chain, Kratky and Porod indicated how a similar crossover point could be obtained from the limiting behavior of the form factor in k -space, measured by scattering [89]. However, this is very difficult to obtain in practice, since the X-ray or neutron scattering needed to probe the relevant length scales often requires concentrations above the overlap concentration to produce sufficient scattering intensity. So the results do not represent only the distribution of scattering centers within independent molecules but also contains contributions from intermolecular distributions (compare with Figure 1.9). There are also practical difficulties associated with determining the location of the crossover point [114].

To summarize, the four classes of persistence length are as follows [90]:

- Bending coefficient, l_{bc}
- Orientational correlation length, l_{oc}
- Crossover distance, l_{cd}
- Projection length, l_p

The bending coefficient is primarily a model parameter, while the rest are observable. However, the orientational correlation length and the crossover distance are only defined given that a molecule behaves in a certain way. Only the projection length is decoupled from any defining model, in the sense that it can always be obtained, for example, from a radius of gyration regardless of the local behavior of the chain. However, this also means that the projection length does not generally say anything about the local behavior. In particular, although equations for the wormlike chain, such as (1.33) and (1.34), can be used to calculate a projection length, there is no need for the chain to be wormlike nor should the results be interpreted as if it were, unless it can be proved that the wormlike chain is a good model for the molecule at hand.

1.5.2 Interactions and the Separation of Length Scales

Having introduced the different definitions of persistence length, we are now ready to substantiate the claim that they represent different properties and are not equivalent (except in the special case of a wormlike chain). Figure 1.11 shows the behavior of the orientational correlation function obtained by simulations of flexible polyelectrolytes, more specifically a model consisting of a freely jointed chain with a fixed bond length b and charged “joints” interacting through a screened Coulomb potential (see Eq. (1.15)). The range of interactions is reduced by decreasing the screening length, κ^{-1} , which corresponds to an increase in the salt concentration.

For a wormlike chain, the semilogarithmic plot of the correlation function would simply be a straight line with slope $-b/l_{oc}$ (see Eq. 1.24) passing through the origin,

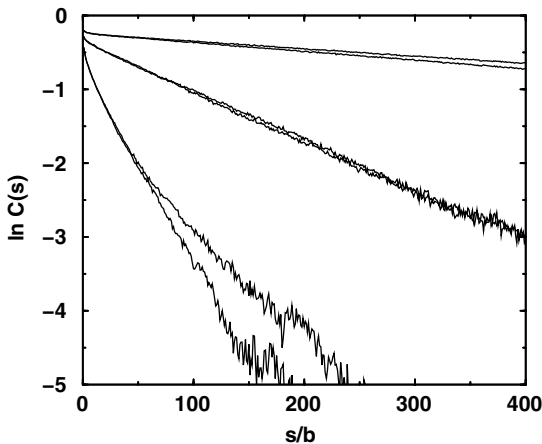


Figure 1.11 Logarithm of the orientational correlation function versus bond separation from Monte Carlo simulations of freely jointed chains ($N \geq 1000$) with screened Coulomb interactions that have a range of 160 and 320 neighboring monomers (*lower* and *upper* curve in each pair, respectively). The fixed bond length is $b = 3 \text{ \AA}$ and the (implicit) concentrations of 1 : 1 salt are, from top to bottom, 0.001 M, 0.01 M, and 0.1 M (the dimensionless screening length, $1/kb$, corresponds to 33, 10, and 3 bonds, respectively).

that is, having an intercept $\ln C_0 = 0$. The curves at the two lowest salt concentration in Figure 1.11 are, to a good approximation, straight lines, but they do not pass through the origin. Instead they have an intercept $\ln C_0 < 0$, which means that while the long-range behavior is wormlike, the short-range behavior represents a more flexible chain. As a consequence, a better expression for the orientational correlation function would be a two-parameter model, dubbed a snakelike chain [90,115,116],

$$C(s) = C_0 e^{-s/l_{oc}}. \quad (1.43)$$

If we insert this into (1.35) and take the infinite chain-limit (see Eq. (1.36)), the result is

$$l_p = \int_0^\infty C_0 e^{-s/l_{oc}} ds = C_0 l_{oc}. \quad (1.44)$$

From Figure 1.11 it is clear that both the slope and the intercept change with salt concentration, that is, both C_0 and l_{oc} are functions of the salt concentration, and l_p must have a different salt dependence than l_{oc} alone. In other words, the projection length and the orientational correlation length are not the same molecular property. Furthermore, if we similarly apply the snakelike chain to calculate the mean-square radius of gyration and end-to-end distance as in (1.32) and (1.39) and take the long-chain limit, we get

$$R_G^2 = \frac{C_0 l_{oc} L}{3} = \frac{l_p L}{3}, \quad (1.45)$$

and

$$R_{ee}^2 = 2LC_0l_{oc} = 2Ll_p, \quad (1.46)$$

respectively, also using (1.44). The conclusion is that if we were to use these equations to calculate a persistence length from R_G or R_{ee} , we would get the projection length as defined in (1.44). Although the snakelike chain is also a simplification and is not expected to hold for real molecules in general, as we will see in a moment, it does illustrate a difference between different definitions of persistence length and the rationale for lumping together definitions that involve integration (implicitly) over the orientational correlation function.

The problem with the wormlike chain is that it only has one parameter. As we have seen, we need at least two parameters to describe the chain behavior because of the separation of length scales. As a conformational measure the projection length represents a combination of different effects, but since it is also a single value, it hides the details.

The separation of length scales is also addressed by the blob model [117,118]. A blob is defined as a segment of the chain that is large enough to have a total electrostatic interaction on the order of $1 k_B T$ with the next segment of the same size. The behavior within a blob (i.e., the short-range behavior) is assumed to be that of a freely jointed chain. These two conditions give the size of a blob. Above the blob size, the molecule is represented as a chain of blobs. After a chain has been rescaled with the blob size determined by the theory, the chain of blobs is normally treated in the usual one-parameter fashion. It can be shown [90] that the snakelike chain also corresponds to a rescaled chain, but instead of representing the shortest length scales as a random walk, each bond has on average a preferred direction, which changes along the chain like an effective wormlike chain; this is equivalent to a model proposed by Barrat and Joanny [119]. Although the random-walk approximation may not be entirely correct, it does give the blob model a predictive capability that is lacking in the snakelike chain. The latter remains an empirical model whose parameter values can only be obtained by measuring the orientational correlation function. This is easy in simulations, but experimentally accessible only under certain circumstances, such as the measurements of DNA on supporting grids or surfaces [93–95,97].

The resemblance of a general chain to a wormlike chain, or more precisely to a snakelike chain, only exists when the chain is semiflexible, meaning as long as it is stiff enough to never be able to bend around and bite its tail. When the chain is so flexible that distant parts of the chain are able to get close and interact occasionally, we get so-called excluded volume effects. This is manifested as extra long-range correlations, as can be seen in Figure 1.11 in the curve bending up and away from an imagined straight line and in the difference between chains with 160 and 320 interacting monomers. When the logarithm of the correlation function is no longer a linear function, meaning $C(s)$ is no longer exponential, l_{oc} is not defined anymore but l_p still is, at least as long as the chain is finite. However, the projection length becomes chain-length dependent (as illustrated by the figure), albeit less so than, for example, R_G .

The strength of the projection length is that it makes different kinds of experimental approaches, as well as some theoretical ones, comparable. Often an experimental

observable can be calculated in the framework of the wormlike chain, and even if the molecule itself is not wormlike, it is possible to treat the projection length obtained by comparing the experimental results to the model calculation as an operational definition. Furthermore, despite differences in techniques such as light scattering and viscosity measurements, the projection lengths obtained in each case are connected through the implied integration over the orientational correlation function. That this connection makes the results comparable is admittedly a conjecture, based on calculations like those for the snakelike chain above and the fact that simulations have shown that different definitions of projection length give the same results, at least qualitatively [115]. The notion is also supported by the fact that experimental results have mostly conformed to one of two kinds of results, attributable to either semiflexible chains or flexible chains with excluded volume effects (see the next section).

1.5.3 Polyelectrolyte Behavior: Electrostatic Persistence Length

Under normal conditions, namely in an aqueous solution with only monovalent ions, a polyelectrolyte expands compared to its unperturbed conformations as a result of the intramolecular electrostatic repulsion. Theoretically this is treated either as an expansion of a freely jointed chain or as a stiffening of a wormlike chain. The earliest polyelectrolyte theories adopted the former view and tried to find a balance between the electrostatic interactions and the chain entropy of a freely jointed chain by minimizing a free energy expressed in terms of the end-to-end distance [120–124]. In its simplest form, this type of calculation is known as the Flory approach [117,125]. There are also more modern theories following in the same tradition [126,127].

The alternate view was pioneered by Odijk [128] and, independently, Skolnick and Fixman [129] (OSF). They performed a perturbation calculation for a rigid rod, bending only slightly so that the electrostatic interactions could be cast in the same form as (1.22) with an electrostatic bending coefficient $l_{bc,e}$. The elastic and electrostatic contributions then become additive so that the total bending coefficient can be written

$$l_{bc} = l_{bc,0} + l_{bc,e}, \quad (1.47)$$

where $l_{bc,0}$ is the intrinsic bending coefficient that describes the bending elasticity in the absence of electrostatic interactions. In the discussion about electrostatic persistence that has followed this work, it has generally been assumed that this additivity, applicable to a rigid rod, holds regardless of the chain stiffness and for any definition of persistence length. In many situations, however, this assumption is of little consequence, such as when the electrostatic interactions are completely dominating or in the reverse case when they are more or less screened out by large amounts of salt.

The result of the perturbation calculation is [128]

$$l_{bc,e} = \frac{(\alpha N)^2 l_B}{12} [3y^{-2} - 8y^{-3} + e^{-y}(y^{-1} + 5y^{-2} + 8y^{-3})], \quad (1.48)$$

where α is the degree of ionization of the N charges and $y \equiv \kappa L$. For large y , this reduces to [128,129]

$$l_{bc,e} = \frac{\alpha^2 l_B}{4\kappa^2 b^2} = \frac{\xi_p}{4\kappa^2 b}, \quad (1.49)$$

where b is the distance between charges (the linear charge density is $\alpha e/b$) and $\xi_p \equiv \alpha^2 l_B/b$ is a coupling parameter that describes the intramolecular electrostatic interactions. Equation (1.49) is a simple power law that describes an electrostatic persistence length that depends quadratically on the screening length. This is how the conclusion of OSF theory is generally expressed, and it has spurred much interest in the calculation of persistence length and the search for power laws in both experiments and theory. OSF theory was derived for a rigid rod, and it has indeed been confirmed for stiff molecules, such as DNA [106,130,131] and poly(xylylene tetrahydrothiophenium chloride) [132]. The same behavior has also been seen in simulations of chains with large intrinsic stiffness [115,133].

However, the question whether the power law of OSF theory also applies to flexible molecules been controversial. Experiments tend to show a different power law behavior, namely a linear dependence on the screening length [134–139], while theory and simulations have produced support for both power laws as well as an argument that there is no power law. The cause of the theoretical diversity is discussed in detail elsewhere [90,115,116,140], but one explanation is the use of different definitions of persistence length. While the cited experiments have consistently reported projection length, theory and simulation studies have variously used all four definitions. In the simulations using the projection length, the results follow the linear power law [90,115,141–143] and in other, more recent simulations it is shown that this power law is coupled to excluded volume effects [116,144,145]. The latter simulations have also demonstrated that for very strong electrostatic interactions, achieved by very long chains (many charges) and long screening lengths (many charges interacting with little screening), flexible polyions can be made stiff enough to exhibit the OSF-type power law behavior.

To summarize the simulation results, it is possible to divide the salt dependence of the electrostatic projection length of flexible polyions into three regimes: an unscreened regime, a semiflexible regime, and an excluded volume regime. As is illustrated in Figure (1.12), this is easily rationalized by considering the relation between the screening length and the chain dimensions, which should also apply to experimental systems.

At a very low ionic strength the screening length is much greater than the chain dimensions, so the polyion can be regarded as unscreened. As long as the screening length remains large compared to the chain size, increasing the salt concentration does not affect the intramolecular interactions and the chain extension is constant, corresponding to its maximum value given the amount of charge on the chain. In the unscreened regime the projection length is therefore constant, independent of the ionic strength.

When the screening length becomes comparable to the chain dimensions, the interactions within the chain start to be screened and the flexibility increases;

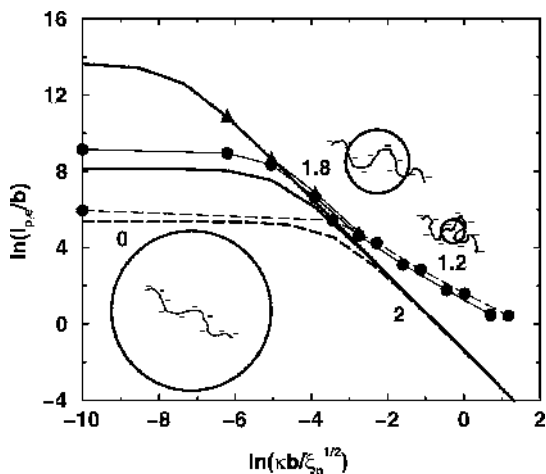


Figure 1.12 The electrostatic projection length as a function of $\kappa b/\xi_p^{1/2}$ for simulations with $\xi_p = 2.4$ (thin solid lines with symbols) with $N = 320$ (circles) and 5000 (triangles), and $\xi_p = 0.15$ with $N = 320$ (thin dashed lines with circles). Points on the y-axis represent the salt-free case ($\kappa = 0$). Otherwise, the dimensionless screening length $(\kappa b)^{-1}$ ranges from 320 down to 0.25 bonds (from left to right). The thick lines without symbols are the predictions of the Odijk expression, equation (1.48), for the three cases. The numbers are the absolute values of the slopes giving the power w of $l_{p,e}/b \sim (\xi_p^{1/2}/\kappa b)^w$, with the simulation results on the right and the OSF values on the left. Also shown are schematic representations of the relation between the chain dimensions and the screening length, where the latter is represented by the radius of the circle for each of the three regimes.

that is to say, the chain dimensions and the projection length start to decrease. If the electrostatic interactions are strong enough to make the chain effectively rodlike in the unscreened regime, the polyion will start to behave as a semiflexible chain. As can be seen in the figure, the persistence length depends nearly quadratically on the screening length, more or less in agreement with OSF theory. The latter deals with a bending coefficient, while the simulation results are for the projection length. If the molecule were truly wormlike, there would be no contradiction, since the definitions are equivalent in this limit. However, in the simulations the chains are more snakelike, in that they show an exponential decay with a varying prefactor (see Figure 1.11 and Eq. (1.43)). This is not exactly what the OSF model describes, though apparently it is close enough as long as the molecules are fairly stiff.

As the ionic strength continues to increase, the chain will become flexible enough to allow distant parts to get close occasionally. In other words, the excluded volume effects become significant and the behavior of the projection length changes to a more linear dependence on the screening length. Odijk and Houwaart [146] have suggested that the behavior in this regime can be described by an excluded volume treatment applied to a chain following the OSF prediction, which in a simple scaling argument

indeed leads to a power law [118,144,145,147]

$$l_p \sim \frac{1}{\kappa^{1.2}} \quad (1.50)$$

in perfect agreement with the simulations displayed in Figure 1.12. More advanced expressions based on the same idea have also been compared to simulations [141,148,149] and experiments [135,136,138,139,141,150]. However, simulations where the excluded volume effects have been removed have revealed that the underlying behavior is not OSF-like [116]. This is a reasonable result, since the chain in this regime is too flexible to be modeled as a rod. There is still no model that reflects an understanding of the internal conformational behavior of flexible chains in the excluded volume regime.

1.5.4 DNA Persistence Length

DNA is one of the most studied molecules with respect to persistence length. This is not only because of its biological significance but also because it lends itself to be studied by a large variety of methods. Also, being a biomolecule, DNA can be obtained as well-defined, essentially monodisperse samples. We have already touched on the point that as far as molecules go, DNA is rather stiff even when the electrostatic interactions are made negligible by very high salt concentrations. There is a general consensus that the intrinsic persistence length is about 500 Å. This (allowing for values of circa 450–500 Å) has been reported as the value at high salt concentrations in studies using electron microscopy [93], transient electrical birefringence (TEB) [151,152], flow dichroism [130], flow birefringence [153], and force-measuring laser tweezers [106,107]. Maret and Weill found a plateau value of 670 Å from magnetic birefringence data [131] but argued that the large uncertainties in approximate values for certain molecular properties used in the calculation of persistence length, and the fact that the values were lower limits, made the result consistent with the expected intrinsic persistence length of 500 Å.

In contrast, light scattering tends to give lower values, 300 to 400 Å [154–156] and so have extrapolated transient electrical dichroism (TED) results [157], force-extension measurements (in the presence of small amounts of di- and trivalent cations) [105], and fluorescence microscopy [158]. The low values obtained in the early light-scattering measurements [154,155] were dismissed in an overview [159] on the ground that a correction for excluded volume effects was used, which does lower the value but not that much [160].

A recalculation [153] using flow birefringence data obtained earlier [161] also gave high-salt values of the persistence length in the lower range. However, faced with a discrepancy with a newer data set (giving values closer to 500 Å), the authors argued that the difference could be a molecular-weight effect, but also that the newer set was to be preferred, because it was more consistent when using different data analysis procedures [153]. Nevertheless, the results from both data sets hinge on the value for the local anisotropy, which is uncertain. In the studies a choice was made to calibrated the value against other persistence length data to facilitate

comparison. If instead an independent estimate is used in the analysis, the flow birefringence data can give an intrinsic persistence length in the lower range in both cases [160].

Also the electrooptical measurements, originally used to support $l_{p,0} = 500 \text{ \AA}$, are embedded with large uncertainties. The general approach to obtaining a persistence length from TEB and TED is to measure a relaxation time as a function of chain length and fit the results to a model, where persistence length is one of the fitting parameters. There are several models to choose from: the weakly bending rod model [162], a simulation-derived correction for flexibility [163] combined with rigid-rod theories [164–169], and an expression obtained from a similar simulation approach [170]. A problem is that the models give systematically different results [157,169,171]. They are also very sensitive to the parameter values. This sensitivity is sometimes seen as an advantage, but it also means that small fluctuations in the experimental data can have a large impact on the result of the fitting. Furthermore the range of chain lengths used in the fitting changes the results [152,171], even when staying within the proposed range of validity of the models, which is probably partly due to an oversimplification of the model description. It is thus small wonder that the electrooptical studies have been so consistent in producing a value for the intrinsic persistence length of DNA despite large variations in the determining factors. If one instead tries to treat the literature data consistently, the results scatter in all directions [160].

The bottom line is that the experimental value for DNA persistence length is both model and method dependent, and the established value of the intrinsic persistence length, about 500 \AA , is not as exact as has sometimes been proclaimed. It might be fine as a rough estimate, but until a definite definition and a consistent method of determination have been decided, we will have to contend with the fact that any value in the range 300 to 500 \AA can be valid. The exact value of the DNA persistence length will be more a reflection of how it was obtained than a strict representation of the theoretical concept we would like to assign to it.

A similar method dependence seems to apply to the power laws that may exist for the salt dependence of the persistence length [160], although in this case it is clearer what to expect. Regardless of the exact value of the intrinsic persistence length, the conclusion is that DNA is rather stiff, which means that the wormlike chain seem to be appropriate as a first approximation for DNA of moderate length up to a few persistence lengths. Electron microscopy and AFM can be used to measure the local behavior of DNA. Under weakly adsorbing conditions DNA may be assumed to behave as an equilibrated chain on a flat surface. So based on plots of the orientational correlation function or comparisons of the end-to-end distances of subchains with a wormlike chain whose persistence length is obtained from the local curvature, DNA has been shown to be wormlike up to contour lengths of about $5l_{oc}$ and to have a universal behavior that extends even further [93–96,98]. Technically the orientational correlation length l_{oc} was measured, but the results were presented as the bending coefficient l_{bc} to yield values directly comparable to measurements of DNA that is free in (three-dimensional) solution on the assumption that (1.22) is applicable. This means that the reported validity was $10 l_{bc}$, since $l_{oc} = 2l_{bc}$ for this chain model on a two-dimensional surface (see the discussion above).

For short DNA which is fairly rodlike, OSF theory can be expected to hold for the salt dependence of the electrostatic persistence length, as has been observed [106,130,131]. For very long DNA, excluded volume effects become important for the projection length and its dependence on the screening length should become linear instead of quadratic in accord with experiments on flexible polyelectrolytes [134–139] and with simulations [90, 115–116, 141–145]. This was confirmed by measurements on giant T4 DNA [158]. An analysis of light-scattering data [154,156] even shows a sublinear dependence [160]. However, excluded volume effects may influence the results of different methods to a varying degree, and a crossover from a semiflexible regime to an excluded volume regime may show up at different chain lengths or not at all. For example, a stretching experiment perturbs the DNA and may in the stretching itself reduce the occurrence of long-range contacts, thereby reducing the excluded volume effects or even eliminating them, while light scattering just observes DNA free in solution without any external interaction, apart from the bouncing of photons.

REFERENCES

- [1] L. Guldbrand, B. Jönsson, H. Wennerström, P. Linse. Electrical double layer forces. A Monte Carlo study. *J. Chem. Phys.* 80 (1984): 2221–2228.
- [2] L. Guldbrand, L. Nilsson, L. Nordenskiöld. A Monte Carlo simulation study of electrostatic forces between hexagonally packed DNA double helices. *J. Chem. Phys.* 85 (1986): 6686–6699.
- [3] L. Guldbrand, L. Nilsson, L. Nordenskiöld. Erratum: A Monte Carlo simulation study of electrostatic forces between hexagonally packed DNA double helices [*J. Chem. Phys.* 85, 6686 (1986)]. *J. Chem. Phys.* 90 (1989): 5893–5893.
- [4] R. Kjellander, S. Marčelja. Correlation and image charge effects in electric double-layers. *Chem. Phys. Lett.* 112 (1984): 49–53.
- [5] R. Kjellander, S. Marčelja. Inhomogeneous Coulomb fluids with image interactions between planar surfaces. I. *J. Chem. Phys.* 82 (1985): 2122–2135.
- [6] J. P. Valleau, R. Ivkov, G. M. Torrie. Colloid stability: The forces between charged surfaces in an electrolyte. *J. Chem. Phys.* 95 (1991): 520–532.
- [7] I. Rouzina, V. A. Bloomfield. Macroion attraction due to electrostatic correlation between screening counterions. I. Mobile surface-adsorbed ions and diffuse ion cloud. *J. Phys. Chem.* 100 (1996): 9977–9989.
- [8] M. O. Khan, B. Jönsson. Electrostatic correlations fold DNA. *Biopolymers* 49 (1999): 121–125.
- [9] M. O. Khan, S. M. Mel'nikov, B. Jönsson. Anomalous salt effects on DNA conformation: Experiment and theory. *Macromolecules* 32 (1999): 8836–8840.
- [10] B. Jönsson, H. Wennerström, When ion–ion correlations are important in charged colloidal systems. In: C. Holm, P. Kékicheff, R. Podgornik, eds. *Electrostatic Effects in Soft Matter and Biophysics*, Kluwer Academic, Dordrecht, 2001, pp. 171–204.
- [11] L. C. Gosule, J. A. Schellman. Compact form of DNA induced by spermidine. *Nature* 259 (1976): 333–335.

- [12] L. C. Gosule, J. A. Schellman. DNA condensation with polyamines I. Spectroscopic studies. *J. Mol. Biol.* 121 (1978): 311–326.
- [13] D. K. Chatteraj, L. C. Gosule, J. A. Schellman. DNA condensation with polyamines II. Electron microscopic studies. *J. Mol. Biol.* 121 (1978): 327–337.
- [14] R. W. Wilson, V. A. Bloomfield. Counterion-induced condensation of deoxyribonucleic acid: A light-scattering study. *Biochemistry* 18 (1979): 2192–2196.
- [15] J. Widom, R. L. Baldwin. Cation-induced toroidal condensation of DNA studies with $\text{Co}^{3+}(\text{NH}_3)_6$. *J. Mol. Biol.* 144 (1980): 431–453.
- [16] S. A. Allison, J. C. Herr, J. M. Schurr. Structure of viral ϕ 29 DNA condensed by simple triamines: A light-scattering and electron-microscopy study. *Biopolymers* 20 (1981): 469–488.
- [17] J. A. Subirana, J. L. Vives. The precipitation of DNA by spermine. *Biopolymers* 20 (1981): 2281–2283.
- [18] T. J. Thomas, V. A. Bloomfield. Collapse of DNA caused by trivalent cations: pH and ionic specificity effects. *Biopolymers* 22 (1983): 1097–1106.
- [19] J. Widom, R. L. Baldwin. Monomolecular condensation of λ -DNA induced by cobalt hexamine. *Biopolymers* 22 (1983): 1595–1620.
- [20] K. Yoshikawa, M. Takahashi, V. V. Vasilevskaya, A. R. Khokhlov. Large discrete transition in a single DNA molecule appears continuous in the ensemble. *Phys. Rev. Lett.* 76 (1996): 3029–3031.
- [21] M. Takahashi, K. Yoshikawa, V. V. Vasilevskaya, A. R. Khokhlov. Discrete coil–globule transition of single duplex DNAs induced by polyamines. *J. Phys. Chem. B* 101 (1997): 9396–9401.
- [22] Y. Yamasaki, Y. Teramoto, K. Yoshikawa. Disappearance of the negative charge in giant DNA with a folding transition. *Biophys. J.* 80 (2001): 2823–2832.
- [23] S. Takagi, K. Tsumoto, K. Yoshikawa. Intra-molecular phase segregation in a single polyelectrolyte chain. *J. Chem. Phys.* 114 (2001): 6942–6949.
- [24] K. Yoshikawa, Y. Yoshikawa, T. Kanbe. All-or-none folding transition in giant mammalian DNA. *Chem. Phys. Lett.* 354 (2002): 354–359.
- [25] C. W. Tabor, H. Tabor. Polyamines. *Annu. Rev. Biochem.* 53 (1984): 749–790.
- [26] H. M. Wallace, A. V. Fraser, A. Hughes. A perspective of polyamine metabolism. *Biochem. J.* 376 (2003): 1–14.
- [27] P. G. Arscott, C. Ma, J. R. Wenner, V. A. Bloomfield. DNA condensation by cobalt hexaammine(III) in alcohol–water mixtures: Dielectric constant and other solvent effects. *Biopolymers* 36 (1995): 345–365.
- [28] K. Yoshikawa, S. Kidoaki, M. Takahashi, V. V. Vasilevskaya, A. R. Khokhlov. Marked discreteness on the coil–globule transition of single duplex DNA. *Ber. Bunsen-Ges. Phys. Chem.* 100 (1996): 876–880.
- [29] S. He, P. G. Arscott, V. A. Bloomfield. Condensation of DNA by multivalent cations: Experimental studies of condensation kinetics. *Biopolymers* 53 (2000): 329–341.
- [30] J. J. Schweinefus, V. A. Bloomfield. The greater negative charge density of DNA in tris-borate buffers does not enhance DNA condensation by multivalent cations. *Biopolymers* 54 (2000): 572–577.

- [31] B. I. Kankia, V. Buckin, V. A. Bloomfield. Hexamminecobalt(III)-induced condensation of calf thymus DNA: Circular dichroism and hydration measurements. *Nucleic. Acids Res.* 29 (2001): 2795–2801.
- [32] Y. Yamasaki, K. Yoshikawa. Higher order structure of DNA controlled by the redox state of $\text{Fe}^{2+}/\text{Fe}^{3+}$. *J. Am. Soc.* 119 (1997): 10573–10578.
- [33] R. M. Fuoss, A. Katchalsky, S. Lifson. The potential of an infinite rod-like molecule and the distribution of the counter ions. *Proc. Natl. Acad. Sci. USA* 37 (1951): 579–589.
- [34] T. Alfrey Jr., P. W. Berg, H. Morawetz. The counterion distribution in solutions of rod-shaped polyelectrolytes. *J. Polym. Sci.* 7 (1951): 543–547.
- [35] M. Ullner, G. Staikos, D. N. Theodorou. Monte Carlo simulations of a single polyelectrolyte in solution: Activity coefficients of the simple ions and application to viscosity measurements. *Macromolecules* 31 (1998): 7921–7933.
- [36] R. M. Davis, W. B. Russel. Intrinsic viscosity and Huggins coefficient for potassium poly(styrenesulfonate) solutions. *Macromolecules* 20 (1987): 518–525.
- [37] G. Staikos, G. Bokias. The intrinsic viscosity of poly(acrylic acid) and partially neutralized poly(acrylic acid) by isoionic dilution. *Polym. Int.* 31 (1993): 385–389.
- [38] G. Bokias, G. Staikos. A quantitative description of the viscometric behaviour of partially neutralized poly(acrylic acid) in aqueous solutions studied by the isoionic dilution method. *Polymer* 36 (1995): 2079–2082.
- [39] Y. Mylonas, G. Staikos, M. Ullner. Chain conformation and intermolecular interaction of partially neutralized poly(acrylic acid) in dilute aqueous solutions. *Polymer* 40 (1999): 6841–6847.
- [40] C. W. Outhwaite. A modified Poisson-Boltzmann equation for the ionic atmosphere around a cylindrical wall. *J. Chem. Soc., Faraday Trans. 2* 82 (1986): 789–794.
- [41] L. B. Bhuiyan, C. W. Outhwaite. A modified Poisson–Boltzmann treatment of an isolated cylindrical electric double layer, In: L. Blum, F. B. Malik, eds. *Condensed Matter Theories*, Vol. 8, Plenum, New York, 1993, pp. 551–559.
- [42] L. B. Bhuiyan, C. W. Outhwaite. The cylindrical electric double layer in the modified Poisson–Boltzmann theory. *Philos. Mag. B* 69 (1994): 1051–1058.
- [43] T. Das, D. Bratko, L. B. Bhuiyan, C. W. Outhwaite. Modified Poisson–Boltzmann theory applied to linear polyelectrolyte solutions. *J. Phys. Chem.* 99 (1995): 410–418.
- [44] P. Debye, E. Hückel. Zur Theorie der Elektrolyte. *Phys. Z.* 24 (1923): 185–206.
- [45] T. L. Hill. Approximate calculations of the electrostatic free energy of nucleic acids and other cylindrical macromolecules. *Arch. Biochem. Biophys.* 57 (1955): 229–239.
- [46] D. Stigter. The charged colloidal cylinder with a Gouy double layer. *J. Coll. Int. Sci.* 53 (1975): 296–306.
- [47] G. S. Manning. Limiting laws and counterion condensation in polyelectrolyte solutions I. Colligative properties. *J. Chem. Phys.* 51 (1969): 924–933.
- [48] G. S. Manning. Limiting laws and counterion condensation in polyelectrolyte solutions. IV. The approach to the limit and the extraordinary stability of the charge fraction. *Biophys. Chem.* 7 (1977): 95–102.
- [49] G. S. Manning. Limiting laws and counterion condensation in polyelectrolyte solutions. V. Further development of the chemical model. *Biophys. Chem.* 9 (1978): 65–70.

- [50] G. S. Manning. Counterion binding in polyelectrolyte theory. *Acc. Chem. Res.* 12 (1979): 443–449.
- [51] G. E. Kimball, M. Cutler, H. Samelson. A theory of polyelectrolytes. *J. Phys. Chem.* 56 (1952): 57–60.
- [52] T. L. Hill. Size and shape of polyelectrolyte molecules in solution. *J. Chem. Phys.* 20 (1952): 1173–1174.
- [53] P. J. Flory. Molecular configuration of polyelectrolytes. *J. Chem. Phys.* 21 (1953): 162–163.
- [54] F. Oosawa, N. Imai, I. Kagawa. Theory of strong polyelectrolyte solutions. I. Coiled macro ions. *J. Polym. Sci.* 13 (1954): 93–111.
- [55] F. Oosawa, N. Imai. Note on solutions of linear polyelectrolyte molecules. *J. Chem. Phys.* 22 (1954): 2084–2085.
- [56] F. Oosawa. A simple theory of thermodynamic properties of polyelectrolyte solutions. *J. Polym. Sci.* 23 (1957): 421–430.
- [57] G. S. Manning. Comments on “A comparison of Manning’s polyelectrolyte theory with the cylindrical Gouy model” by D. Stigter. *J. Phys. Chem.* 82 (1978): 2349–2351.
- [58] D. Stigter. A comparison of Manning’s polyelectrolyte theory with the cylindrical Gouy model. *J. Phys. Chem.* 82 (1978): 1603–1606.
- [59] M. Fixman. The Poisson–Boltzmann equation and its application to polyelectrolytes. *J. Chem. Phys.* 70 (1979): 4995–5005.
- [60] M. Guéron, M. Weisbuch. Polyelectrolyte theory. I. Counterion accumulation, site-binding, and their insensitivity to polyelectrolyte shape in solutions containing finite salt concentrations. *Biopolymers* 19 (1980): 353–382.
- [61] D. Stigter. Evaluation of the counterion condensation theory of polyelectrolytes. *Biophys. J.* 69 (1995): 380–388.
- [62] G. S. Manning. The critical onset of counterion condensation: A survey of its experimental and theoretical basis. *Ber. Bunsen–Ges. Phys. Chem.* 100 (1996): 909–922.
- [63] G. S. Manning, J. Ray. Counterion condensation revisited. *J. Biomol. Struct. Dyn.* 16 (1998): 461–476.
- [64] G. S. Manning, A. Holtzer. Application of polyelectrolyte limiting laws to potentiometric titration. *J. Phys. Chem.* 77 (1973): 2206–2212.
- [65] G. S. Manning. Limiting laws and counterion condensation in polyelectrolyte solutions. 6. Theory of the titration curve. *J. Phys. Chem.* 85 (1981): 870–877.
- [66] G. S. Manning. The molecular theory of polyelectrolyte solutions with applications to the electrostatic properties of polynucleotides. *Q. Rev. Biophys.* 11 (1978): 179–246.
- [67] C. Ma, V. A. Bloomfield. Gel electrophoresis measurement of counterion condensation on DNA. *Biopolymers* 35 (1995): 211–216.
- [68] M. L. Huggins. The viscosity of dilute solutions of long-chain molecules. IV. Dependence on concentration. *J. Am. Chem. Soc.* 64 (1942): 2716–2718.
- [69] P. J. Flory. *Principles of Polymer Chemistry*, Cornell University Press, Ithaca, NY, 1953.
- [70] H. Yamakawa. *Modern Theory of Polymer Solutions*, Harper and Row, New York, 1971.
- [71] W. B. Russel. The low-shear limit of the effective viscosity of a solution of charged macromolecules. *J. Fluid. Mech.* 80 (1979): 401–419.

- [72] H. Eisenberg, J. Pouyet. Viscosities of dilute aqueous solutions of a partially quarter-nized poly-4-vinylpyridine at low gradients of flow. *J. Polym. Sci.* 13 (1954): 85–91.
- [73] H. Terayama, F. T. Wall. Reduced viscosities of polyelectrolytes in the presence of added salts. *J. Polym. Sci.* 16 (1955): 357–365.
- [74] R. M. Fuoss. Viscosity function for polyelectrolytes. *J. Polym. Sci.* 3 (1948): 604–604.
- [75] R. M. Fuoss, U. P. Strauss. The viscosity of mixtures of polyelectrolytes and simple electrolytes. *Ann. NY Acad. Sci.* 51 (1949): 836–851.
- [76] F. Eirich. General discussion. *Discuss. Faraday Soc.* 11 (1952): 153–153.
- [77] S. Förster, M. Schmidt. Polyelectrolytes in solution. *Adv. Polym. Sci.* 120 (1995): 51–133.
- [78] R. A. Mock, C. A. Marshall. Vinyltoluene-styrene copolymer sulfonic acid. I. Viscous properties and ionic character in hydrochlorid acid solutions. *J. Polym. Sci.* 13 (1954): 263–277.
- [79] J. Cohen, Z. Priel. Intrinsic viscosity of polyelectrolyte solutions. *Polym. Comm.* 30 (1989): 223–224.
- [80] B. Rosen, P. Kamath, F. Eirich. General discussion. *Discuss. Faraday Soc.* 11 (1952): 135–147.
- [81] J. Cohen, Z. Priel, Y. Rabin. Viscosity of dilute polyelectrolyte solutions. *J. Chem. Phys.* 88 (1988): 7111–7116.
- [82] J. Yamanaka, H. Matsuoka, H. Kitano, N. Ise, T. Yamaguchi, S. Saeki, M. Tsubokawa. Revisit to the intrinsic viscosity-molecular weight relationship of ionic polymers. 3. Viscosity behavior of ionic polymer latices in ethylene glycol/water mixtures. *Langmuir* 7 (1991): 1928–1934.
- [83] J. Yamanaka, S. Yamada, N. Ise, T. Yamaguchi. Revisit to the intrinsic viscosity-molecular weight relationship of ionic polymers. 7. Examination of the Pals–Hermans dilution method with reference to the viscosity behavior of dilute aqueous dispersion of ionic polymer latex. *J. Polym. Sci., Polym. Phys. Ed.* 33 (1995): 1523–1526.
- [84] J. Wu, Y. Wang, M. Hara, M. Granville, R. J. Jerome, Salt-free polyelectrolyte behavior of polystyrene-based telechelic ionomers in a polar solvent. I. Viscosity and low-angle light scattering studies. *Macromolecules* 27 (1994): 1195–1200.
- [85] M. Antonietti, A. Briel, S. Förster. Intrinsic viscosity of small spherical polyelectrolytes: Proof of the intermolecular origin of the polyelectrolyte effect. *J. Chem. Phys.* 105 (1996): 7795–7807.
- [86] D. T. F. Pals, J. J. Hermans. New method for deriving the intrinsic viscosity of polyelectrolytes. *J. Polym. Sci.* 5 (1950): 733–734.
- [87] D. T. F. Pals, J. J. Hermans. Sodium salts of pectin and of carboxy methyl cellulose in aqueous sodium chloride. I. Viscosities. *Recl. Trav. Chim. Pays-Bas* 71 (1952): 433–457.
- [88] L. D. Landau, E. M. Lifshitz. *Statistical Physics*, 2nd ed., Pergamon Press, Oxford, 1970.
- [89] O. Kratky, G. Porod. Röntgenuntersuchung gelöster Fadenmoleküle. *Recl. Trav. Chim. Pays-Bas* 68 (1949): 1106–1122.
- [90] M. Ullner, C. E. Woodward. Orientational correlation function and persistence lengths of flexible polyelectrolytes. *Macromolecules* 35 (2002): 1437–1445.

- [91] A. Y. Grosberg, A. R. Khokhlov. *Statistical Physics of Macromolecules*, AIP Press, New York, 1994.
- [92] N. Saitô, K. Takahashi, Y. Yunoki. The statistical mechanical theory of stiff chains. *J. Phys. Soc. Jpn.* 22 (1967): 219–226.
- [93] C. Frontali, E. Dore, A. Ferrauto, E. Gratton, A. Bettini, M. R. Pozzan, E. Valdevit. An absolute method for the determination of the persistence length of native DNA from electron micrographs. *Biopolymers* 18 (1979): 1353–1373.
- [94] C. Rivetti, M. Guthold, C. Bustamante. Scanning force microscopy of DNA deposited onto mica: Equilibration *versus* kinetic trapping studied by statistical polymer chain analysis. *J. Mol. Biol.* 264 (1996): 919–932.
- [95] A. Podestà, M. Indrieri, D. Brogioli, G. S. Manning, P. Milani, R. Guerra, L. Finzi, D. Dunlap. Positively charged surfaces increase the flexibility of DNA. *Biophys. J.* 89 (2005): 2558–2563.
- [96] A. Bettini, M. R. Pozzan, E. Valdevit, C. Frontali. Microscopic persistence length of native DNA: Its relation to average molecular dimensions. *Biopolymers* 19 (1980): 1689–1694.
- [97] M. Joanicot, B. Revet. DNA conformational studies from electron microscopy. I. excluded volume effect and structure dimensionality. *Biopolymers* 26 (1987): 315–326.
- [98] C. Frontali. Excluded-volume effect on the bidimensional conformation of DNA molecules adsorbed to protein films. *Biopolymers* 27 (1988): 1329–1331.
- [99] J. Bednar, P. Furrer, V. Katritch, A. Z. Stasiak, J. Dubochet, A. Stasiak. Determination of DNA persistence length by cryo-electron microscopy. Separation of the static and dynamic contributions to the apparent persistence length of DNA. *J. Mol. Biol.* 254 (1995): 579–594.
- [100] B. T. Stokke, D. A. Brant. The reliability of wormlike polysaccharide chain dimensions estimated from electron micrographs. *Biopolymers* 30 (1990): 1161–1181.
- [101] S. B. Smith, L. Finzi, C. Bustamante. Direct mechanical measurements of the elasticity of single DNA molecules by using magnetic beads. *Science* 258 (1992): 1122–1126.
- [102] C. Bustamante, J. F. Marko, E. D. Siggia, S. Smith. Entropic elasticity of λ -phage DNA. *Science* 265 (1994): 1599–1600.
- [103] T. T. Perkins, D. E. Smith, R. G. Larson, S. Chu. Stretching of a single tethered polymer in a uniform flow. *Science* 268 (1995): 83–87.
- [104] S. B. Smith, Y. Cui, C. Bustamante. Overstretching B-DNA: The elastic response of individual double-stranded and single stranded DNA molecules. *Science* 271 (1996): 795–799.
- [105] M. D. Wang, H. Yin, R. Landick, J. Gelles, S. M. Block. Stretching DNA with optical tweezers. *Biophys. J.* 72 (1997): 1335–1346.
- [106] C. G. Baumann, S. B. Smith, V. A. Bloomfield, C. Bustamante. Ionic effects on the elasticity of single DNA molecules. *Proc. Natl. Acad. Sci. USA.* 94 (1997): 6185–6190.
- [107] C. G. Baumann, V. A. Bloomfield, S. B. Smith, C. Bustamante, M. D. Wang, S. M. Block. Stretching of single collapsed DNA molecules. *Biophys. J.* 78 (2000): 1965–1978.
- [108] A. V. Vologodskii. DNA extension under the action of an external force. *Macromolecules* 27 (1994): 5623–5625.
- [109] T. Odijk. Stiff chains and filaments under tension. *Macromolecules* 28 (1995): 7016–7018.
- [110] J. F. Marko, E. D. Siggia. Stretching DNA. *Macromolecules* 28 (1995): 8759–8770.

- [111] B.-Y. Ha, D. Thirumalai. Semiflexible chains under tension. *J. Chem. Phys.* 106 (1997): 4243–4247.
- [112] R. Podgornik, P. L. Hansen, V. A. Parsegian. Elastic moduli renormalization in self-interacting stretchable polyelectrolytes. *J. Chem. Phys.* 113 (2000): 9343–9350.
- [113] C. Bustamante, S. B. Smith, J. Liphard, D. Smith. Single-molecule studies of DNA mechanics. *Curr. Opin. Struct. Biol.* 10 (2000): 279–285.
- [114] S. Förster, M. Schmidt. Polyelectrolytes in solution. *Adv. Polym. Sci.* 120 (1995): 51–133.
- [115] M. Ullner, B. Jönsson, C. Peterson, O. Sommelius, B. Söderberg. The electrostatic persistence length calculated from Monte Carlo, variational and perturbation methods. *J. Chem. Phys.* 107 (1997): 1279–1287.
- [116] M. Ullner. Comments on the scaling behavior of flexible polyelectrolytes within the Debye–Hückel approximation. *J. Phys. Chem. B* 107 (2003): 8097–8110.
- [117] P. G. de Gennes, P. Pincus, R. M. Velasco, F. Brochard. Remarks on polyelectrolyte conformation. *J. Phys. (Paris)* 37 (1976): 1461–1473.
- [118] A. R. Khokhlov, K. A. Khachaturian. On the theory of weakly charged polyelectrolytes. *Polymer* 23 (1982): 1742–1750.
- [119] J.-L. Barrat, J.-F. Joanny. Persistence length of polyelectrolyte chains. *Europhys. Lett.* 24 (1993): 333–338.
- [120] J. J. Hermans, J. T. G. Overbeek. The dimensions of charged long chain molecules in solutions containing electrolytes. *Recl. Trav. Chim. Pays-Bas* 67 (1948): 761–776.
- [121] W. Kuhn, O. Künzle, A. Katchalsky. Verhalten polyvalenter Fadenmolekelionen in Lösung. *Helv. Chim. Acta* 31 (1948): 1994–2037.
- [122] A. Katchalsky, O. Künzle, W. Kuhn. Behavior of polyvalent polymeric ions in solution. *J. Polym. Sci.* 5 (1950): 283–300.
- [123] A. Katchalsky, S. Lifson. The electrostatic free energy of polyelectrolyte solutions. I. Randomly kinked macromolecules. *J. Polym. Sci.* 11 (1953): 409–423.
- [124] F. E. Harris, S. A. Rice. The random chain model for polyelectrolytes. *J. Polym. Sci.* 15 (1955): 151–156.
- [125] M. E. Fisher. Comment to “Statistics of long chains with repulsive interactions” by J. des Cloizeaux. *J. Phys. Soc. Jpn.*, suppl. 26 (1969): 44–45.
- [126] M. Muthukumar. Adsorption of a polyelectrolyte chain to a charged surface. *J. Chem. Phys.* 86 (1987): 7230–7235.
- [127] M. Muthukumar. Double screening in polyelectrolyte solutions: Limiting laws and crossover formulas. *J. Chem. Phys.* 105 (1996): 5183–5199.
- [128] T. Odijk. Polyelectrolytes near the rod limit. *J. Polym. Sci., Polym. Phys. Ed.* 15 (1977): 477–483.
- [129] J. Skolnick, M. Fixman. Electrostatic persistence length of a wormlike polyelectrolyte. *Macromolecules* 10 (1977): 944–948.
- [130] V. Rizzo, J. Schellman. Flow dichroism of T7 DNA as a function of salt concentration. *Biopolymers* 20 (1981): 2143–2163.
- [131] G. Maret, G. Weill. Magnetic birefringence study of the electrostatic and intrinsic persistence length of DNA. *Biopolymers* 22 (1983): 2727–2744.
- [132] H. Mattoussi, S. O’Donohue, F. E. Karasz. Polyion conformation and second virial coefficient dependences on the ionic strength for flexible polyelectrolyte solutions. *Macromolecules* 25 (1992): 743–749.

- [133] U. Micka, K. Kremer. Persistence length of weakly charged polyelectrolytes with variable intrinsic stiffness. *Europhys. Lett.* 38 (1997): 279–284.
- [134] M. Tricot. Comparison of experimental and theoretical persistence length of some polyelectrolytes at various ionic strengths. *Macromolecules* 17 (1984): 1698–1704.
- [135] S. Ghosh, X. Li, C. E. Reed, W. F. Reed. Apparent persistence lengths and diffusion behavior of high molecular weight hyaluronate. *Biopolymers* 30 (1990): 1101–1112.
- [136] W. F. Reed, S. Ghosh, G. Medjahdi, J. Francois. Dependence of polyelectrolyte apparent persistence lengths, viscosity, and diffusion on ionic strength and linear charge density. *Macromolecules* 24 (1991): 6189–6198.
- [137] V. Degiorgio, F. Mantegazza, R. Piazza. Transient electric birefringence measurement of the persistence length of sodium polystyrene sulfonate. *Europhys. Lett.* 15 (1991): 75–80.
- [138] G. A. Sorci, W. F. Reed. Electrostatically enhanced second and third virial coefficients, viscosity, and interparticle correlations for linear polyelectrolytes. *Macromolecules* 35 (2002): 5218–5227.
- [139] G. A. Sorci, W. F. Reed. Effect of the valence and chemical species of added electrolyte on polyelectrolyte conformations and interactions. *Macromolecules* 37 (2004): 554–565.
- [140] M. Manghi, R. R. Netz. Variational theory for a single polyelectrolyte chain revisited. *Eur. Phys. J. E* 14 (2004): 67–77.
- [141] C. E. Reed, W. F. Reed. Monte Carlo electrostatic persistence lengths compared with experiment and theory. *J. Chem. Phys.* 94 (1991): 8479–8486.
- [142] J.-L. Barrat, D. Boyer. Numerical study of a charged bead-spring chain. *J. Phys. II* 3 (1993): 343–356.
- [143] C. Seidel. Polyelectrolyte simulation. *Ber. Bunsen-Ges. Phys. Chem.* 100 (1996): 757–763.
- [144] R. Everaers, A. Milchev, V. Yamakov. The electrostatic persistence length of polymers beyond the OSF limit. *Eur. Phys. J. E* 8 (2002): 3–14.
- [145] T. T. Nguyen, B. I. Shklovskii. Persistence length of a polyelectrolyte in salty water: Monte Carlo study. *Phys. Rev. E* 66 (2002): 021801.
- [146] T. Odijk, A. C. Houwaart. On the theory of the excluded-volume effect of a polyelectrolyte in a 1–1 electrolyte solution. *J. Polym. Sci., Polym. Phys. Ed.* 16 (1978): 627–639.
- [147] J.-L. Barrat, J.-F. Joanny. Theory of polyelectrolyte solution. *Adv. Chem. Phys.* 94 (1996): 1–66.
- [148] C. E. Reed, W. F. Reed. Monte Carlo test of electrostatic persistence length for short polymers. *J. Chem. Phys.* 92 (1990): 6916–6926.
- [149] C. E. Reed, W. F. Reed. Monte Carlo study of light scattering by linear polyelectrolytes. *J. Chem. Phys.* 97 (1992): 7766–7776.
- [150] E. Fouissac, M. Milas, M. Rinaudo, R. Borsali. Influence of the ionic strength on the dimensions of sodium hyaluronate. *Macromolecules* 25 (1992): 5613–5617.
- [151] J. G. Elias, D. Eden. Transient electrical birefringence study of the persistence length and electrical polarizability of restriction fragments of DNA. *Macromolecules* 14 (1981): 410–419.
- [152] P. J. Hagerman. Investigation of the flexibility of DNA using transient electric birefringence. *Biopolymers* 20 (1981): 1503–1535.

- [153] K. L. Cairney, R. E. Harrington. Flow birefringence of T7 phage DNA: Dependence on salt concentration. *Biopolymers* 21 (1982): 923–934.
- [154] N. Borochoy, H. Eisenberg, Z. Kam. Dependence on DNA conformation on the concentration of salt. *Biopolymers* 20 (1981): 231–235.
- [155] Z. Kam, N. Borochoy, H. Eisenberg. Dependence of laser light scattering of DNA on NaCl concentration. *Biopolymers* 20 (1981): 2671–2690.
- [156] E. S. Sobel, J. A. Harpst. Effects of Na^+ on the persistence length and excluded volume of T7 bacteriophage DNA. *Biopolymers* 31 (1991): 1559–1564.
- [157] D. Porschke. Persistence length and bending dynamics of DNA from electrooptical measurements at high salt concentrations. *Biophys. Chem.* 40 (1991): 169–179.
- [158] N. Makita, M. Ullner, K. Yoshikawa. Conformational change of giant DNA with added salt as revealed by single molecular observation. *Macromolecules* 39 (2006): 6200–6206.
- [159] P. J. Hagerman. Flexibility of DNA. *Ann. Rev. Biophys. Biophys. Chem.* 17 (1988): 265–286.
- [160] M. Ullner, N. Makita, K. Yoshikawa. unpublished manuscript .
- [161] R. E. Harrington. Opticohydrodynamic properties of high-molecular-weight DNA. III. The effects of NaCl concentration. *Biopolymers* 17 (1978): 919–936.
- [162] J. E. Hearst. Rotary diffusion constants of stiff-chain macromolecules. *J. Chem. Phys.* 38 (1963): 1062–1065.
- [163] P. J. Hagerman, B. H. Zimm. Monte Carlo approach to the analysis of the rotational diffusion of wormlike chains. *Biopolymers* 20 (1981): 1481–1502.
- [164] S. Broersma. Rotational diffusion constant of a cylindrical particle. *J. Chem. Phys.* 32 (1960): 1626–1631.
- [165] S. Broersma. Viscous force constant for a closed cylinder. *J. Chem. Phys.* 32 (1960): 1632–1635.
- [166] J. Newman, H. L. Swinney. Hydrodynamic properties of fd virus. *J. Mol. Biol.* 116 (1977): 593–606.
- [167] S. Broersma. Viscous force and torque constants for a cylinder. *J. Chem. Phys.* 74 (1981): 6989–6990.
- [168] M. M. Tirado, J. García de la Torre. Rotational dynamics of rigid, symmetric top macromolecules: Application to circular cylinders. *J. Chem. Phys.* 73 (1980): 1986–1993.
- [169] M. M. Tirado, C. López Martínez, J. García de la Torre. Comparison of the theories for translational and rotational diffusion coefficients of rod-like macromolecules: Application to short DNA fragments. *J. Chem. Phys.* 81 (1984): 2047–2052.
- [170] J. J. García Molina, M. C. López Martínez, J. García de la Torre. Computer simulation of hydrodynamic properties of semiflexible macromolecules: Randomly broken chains, wormlike chains, and analysis of properties of DNA. *Biopolymers* 29 (1990): 883–900.
- [171] Y. Lu, B. Weers, N. C. Stellwagen. DNA persistence length revisited. *Biopolymers* 61 (2002): 261–275.

